2008

THE METASTASIS SUPPRESSOR NM23-H1 IS REQUIRED FOR DNA REPAIR

Mengmeng Yang
University of Kentucky, spryyoung@gmail.com

ABSTRACT OF DISSERTATION

Mengmeng Yang

The Graduate School

University of Kentucky

2008

THE METASTASIS SUPPRESSOR NM23-H1 IS REQUIRED FOR
DNA REPAIR

_____

ABSTRACT OF DISSERTATION
_____

A dissertation submitted in partial fulfillment of the
requirements for the degree of Doctor of Philosophy in the
College of Medicine
at the University of Kentucky

By
Mengmeng Yang

Lexington, Kentucky

Director: Dr. David Kaetzel, Professor of Molecular and Biomedical Pharmacology

Lexington, Kentucky

2008

ABSTRACT OF DISSERTATION

THE METASTASIS SUPPRESSOR NM23-H1 IS REQUIRED FOR DNA REPAIR

NM23-H1 represents the first identified metastasis suppressor, exhibiting reduced expression in breast carcinoma and melanoma, and an ability to inhibit metastatic growth without significant impact on the transformed phenotype. Although its molecular mechanism of action is not fully understood, NM23-H1 possesses at least three enzymatic activities that may mediate metastasis suppressor function. It catalyzes nucleoside diphosphate kinase (NDPK) activity, as well as protein histidine kinase and 3'-5' exonuclease activities. As 3'-5' exonucleases are generally required for maintenance of genomic integrity, this activity represents a plausible mediator to underlie the metastasis suppressor function of NM23-H1 protein. To investigate the relevant activity of NM23-H1 in metastasis suppression, we constructed a panel of NM23-H1 mutant variants with selective enzymatic lesions. Previous studies have identified some key amino acid residues important for the enzymatic characteristics of NM23-H1. However, none of them are selective for disrupting the 3'-5' exonuclease activity. In this study, we show that a substitution of Glu_5 to alanine results in a dramatic, selective loss in 3'-5' exonuclease property without significant affecting other enzymatic activities. To measure the extent to which the exonuclease function opposes mutation and metastasis, NM23-deficient and metastatic cell lines with forced expression of NM23-H1 variants are analyzed in nude mice. In spontaneous metastasis models, NM23-H1 mutants deficient in 3'-5' exonuclease activity significantly disrupt the capacity of metastasis suppression of wild-type protein, indicating that the 3'-5' exonuclease activity of NM23-H1 is necessary for the spontaneous metastasis-suppressing effects. As 3'-5' exonucleases are generally associated with DNA repair process, we have also studied the contributions of yeast NM23 homologue *YNK1* to genomic integrity in *Saccharomyces cerevisiae*. Consistent with an antimutator function, ablation of *YNK1* significantly results in increased mutation rates following exposure to UV irradiation and the alkylating agent methyl methanesulfonate (MMS). The impaired DNA-damage response of *ynk1Δ* cells suggests a role of human homologue NM23 in DNA repair. More evidence is being collected in our laboratory to demonstrate a role for NM23-H1 in maintaining genomic integrity. Collectively, our findings of DNA repair activity of NM23-H1 will contribute to the

understandings of the mechanisms in metastasis suppression and new drug discoveries.

Mengmeng Yang

May 19, 2008

THE METASTASIS SUPPRESSOR NM23-H1 IS REQUIRED FOR
DNA REPAIR

By

Mengmeng Yang

Dr. David M. Kaetzel
Director of Dissertation

Dr. Robert W. Hadley
Director of Graduate Studies

May 19, 2008
Date

RULES FOR THE USE OF DISSERTATION

Unpublished dissertation submitted for the Doctor's degree and deposited in the University of Kentucky Library are as a rule open for inspection, but are to be used only with due regard to the rights of the authors. Bibliographical references may be noted, but quotations or summaries of parts may be published with only permission of the author, and with the usual scholarly acknowledgements.

Extensive copying or publication of the dissertation in whole or in part also requires the consent of the Dean of the Graduate School of the University of Kentucky.

A library that borrows this dissertation for use by its patrons is expected to secure the signature of each user.

<u>Name</u>   <u>Date</u>
_____
_____
_____
_____
_____
_____
_____
_____
_____
_____
_____
_____
_____
_____
_____
_____
_____
_____
_____
_____
_____
_____
_____
_____
_____
_____
_____
_____
_____

DISSERTATION

Mengmeng Yang

The Graduate School

University of Kentucky

2008

THE METASTASIS SUPPRESSOR NM23-H1 IS REQUIRED FOR
DNA REPAIR

_____

DISSERTATION
_____

A dissertation submitted in partial fulfillment of the
requirements for the degree of Doctor of Philosophy in the
College of Medicine
at the University of Kentucky

By

Mengmeng Yang

Lexington, Kentucky

Director: Dr. David Kaetzel, Professor of Molecular and Biomedical Pharmacology

Lexington, Kentucky

2008

<u>Dedicated to</u>

my husband and best friend
Dr. Peng Zhang

and my beloved parents
Mr. Yimin Yang
Mrs. Zhenen Zhang

ACKNOWLEDGEMENT

I would like to thank so many people for their guidance and support during my graduate study. First of all, my deepest appreciation goes to my advisor, Dr. David M. Kaetzel, for his trust, encouragement and patience; for his willingness to challenge me to think deeply about my research project while at the same time give me plenty of room to grow as a scientist.

I sincerely thank the members of my Ph.D. committee: Dr. Rolf Craven, Dr. Susan Kraner, the late Dr. Stephen Zimmer, Dr. John D'Orazio, and Dr. Robert Dickson as the outside examiner. I appreciate your time and energy to attend meetings, my oral exam and graduate seminar. Thank you very much for reading this dissertation and your valuable input. Specially, I thank Dr. Craven for his invaluable advices and instructions on my yeast work.

I also want to thank my colleagues from Kaetzel's lab, both past and present. Dr. Deqin Ma taught me techniques on DNA cleavage assay and protein HPLC purification. Dr. Qingbei Zhang constructed the animal metastasis model and taught me animal injection and animal surgery. Rob McCorkle completed the assays of histidine kinase activity of NM23-H1 mutants. Marian Novak finished the last replication of spontaneous metastasis assay. Kristen Ormerod helped me with animal handling, tissue freezing and sectioning. My dissertation will not be completed without their assistance and hard work.

Expert technical assistance was provided by a group of great people. Many thanks go to Dr. Trevor Creamer and Dr. Veronique Chellgren, for their

TABLE OF CONTENTS

LIST OF TABLES

LIST OF FIGURES

LIST OF FILES

MengmengYangETD. pdf   2.0MB

CHAPTER ONE
INTRODUCTION

1.1.   Cancer Metastasis Progression and Genomic Instability

Tumor metastases arise from the spread of cancer cells from a primary site and form the colonization in distant organs. Most invasive, malignant tumors give rise to tumor metastases by a multi-step process as shown in Figure 1, in which primary cells lose cellular adhesion, increase motility, invade surrounding tissues, disseminate through the bloodstream to distant organs, and proliferate in new locations (Chambers et al., 2002). Each step must be successfully completed to give rise to a metastatic tumor. Tumor metastases, instead of primary tumors, are the cause of 90% of human cancer deaths (Sporn, 1996). To prevent these deaths, better understanding of the processes and mechanisms of tumor invasion and metastasis is essential to identify promising molecular targets for cancer therapy.

Metastasis is an inefficient process, by which millions of cells might be released by a tumor into the circulation, but only a tiny minority of these cells will colonize at a distant organ (Siclari et al., 2006). *In vivo* microscopy and cell-fate analysis have showed that some steps (e.g., invasion and metastatic colonization) of the metastatic process are more inefficient than some other steps (e.g., cells survival in the circulation, arrest in a distant organ and initial extravasation) (Chambers et al., 2002). Metastatic inefficiency is primarily due to the regulation of cancer cell growth in secondary sites. However, due to their genetic instability and heterogeneity, tumors do have a distinct chance to overcome incompatible microenvironments. During tumor progression, many genes gain or lose function allowing a cancer cell to acquire the prerequisites for metastasis such as altered cell adhesion, limitless replication, increased motility and invasion, and anchorage independent growth (Nguyen and Massague, 2007).

Progression of cancer from a less malignant to a more malignant phenotype is well-accepted to be due to inherent genomic instability (Loeb, 1991, 2001). The accumulated genetic and epigenetic changes lead to an increasingly aggressive and treatment-resistant phenotype, and ultimately

metastasis. This idea is supported by evidence that highly metastatic clones from tumor-cell populations had higher mutation rates than non-metastatic clones from the same tumor. For example, spontaneous mutation rates to ouabain resistance measured in six human melanoma cell lines by Luria and Delbrück using fluctuation analysis correlated with the metastatic ability of the cells: moderately and highly metastatic cells showed spontaneous mutation rates 10 to 50 times higher than those of poorly metastatic cells (Bailly et al., 1993). These results provided a direct link between metastasis and genetic instability.

.

Figure 1. Metastasis is a complex, multistep process.

a **In situ** cancer

b Invasion of the tumour border

d Intravasion of the circulatory system
Survival, transport

c Lymphatic spread

e Arrest
Extravasion

f Solitary dormant cells
Occult micrometastases

g Progressive colonization
Angiogenesis
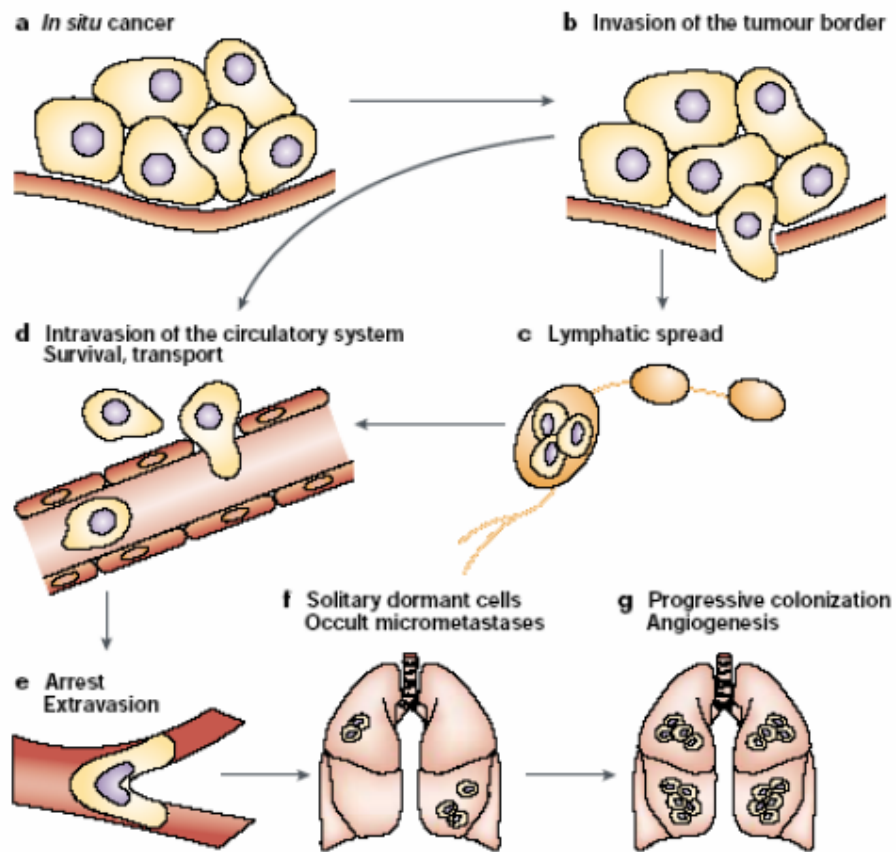
Picture from *2003 Nature Reviews Cancer* **3**, 55 - 63

1.2. NM23 is a Metastasis Suppressor

Metastasis suppressors, by definition, repress metastasis without affecting primary tumor growth. The concept of tumor suppressor prompted the identification of metastasis suppressors, which were found to exhibit reduced expression in highly metastatic tumors or cell lines compared to that of non-metastatic tumor cells (Steeg, 2003). Some other metastasis suppressor genes were cloned when chromosomes or portions of chromosomes were transfected into cell lines and a decrease in metastatic potential was observed. So far, thirteen metastasis suppressor genes have been confirmed (Palmieri et al., 2006). The entire panel of metastasis suppressor genes were validated by re-expression in a metastatic cell line, resulting in inhibition of *in vivo* metastasis without significant effect on tumorigenicity as compared to controls (Steeg, 2003).

Metastasis suppressors often affect many aspects of signal transduction pathways including invasion, growth-factor-receptor signaling, the mitogen-activated protein kinase pathway, cell-cell communication and transcription (Steeg, 2003). For instance, KAI1, a metastasis-suppressor for prostate and breast carcinomas (Dong et al., 1996; Yang et al., 1997), belonging to a tetraspanin family of transmembrane proteins, is directly associated with the EGF receptor and attenuates EGF-induced migration signaling (Odintsova et al., 2000). MKK4, another metastasis-suppressor for prostate and ovary cancer, transduced signals from MEKK1 to stress-activated protein kinase/JNK1 and p38 mitogen-activated protein kinase (Kauffman et al., 2003; Teng et al., 1997). By this mitogen-activated protein kinase pathway, MKK4 regulated the signal transduction of stress-induced apoptosis in cancer (Kim et al., 2001; Yamada et al., 2002).

nm23, the first identified metastasis suppressor gene, represents the most widely validated metastasis suppressor gene based on transfection and knockout mouse strategies. Transfection of *nm23-H1* or *-H2* cDNAs (or their murine homologues *-M1* or *-M2*) into some metastatically competent cell lines can reduce *in vivo* metastatic potential of these cell lines without significant effects on primary tumor formation (Palmieri et al., 2006). These observations were further supported by studies performed in *nm23-M1* knockout mice:

4

when hepatocellular carcinoma was induced into the knockout mice, primary tumor size did not change significantly, whereas the incidence of metastases increased markedly (Boissan et al., 2005). A correlation has been established between low NM23 expression and high metastatic potential in multiple cancers, e.g., melanoma, hepatoma, breast and gastric carcinoma (Hartsough and Steeg, 2000). However, this correlation was absent or opposite in other cancers (e.g., colon carcinoma; (Myeroff and Markowitz, 1993)), suggesting NM23 may play different roles in different tissues.

So far, nine human NM23 members (named as NM23-H1 to -H9) have been reported and were found in multiple subcellular compartments (Lacombe et al., 2000; Sadek et al., 2003). The two most abundantly expressed and the most widely studied, NM23-H1 and NM23-H2, are 88% identical in amino acid sequence. They encode the A and B isoforms of nucleoside diphosphate kinase (NDPK) respectively, catalyzing the transfer of a γ-phosphate between NTPs and NDPs via a "ping-pong" mechanism (Agarwal et al., 1978). The NM23/NDPK genes are highly conserved from prokaryotes to eukaryotes. In addition to NDPK activity, many other biochemical and biological functions were attributed to NM23 proteins, including histidine protein kinase activity (Freije et al., 1997), DNA cleavage activity (Ma et al., 2004; Postel, 1999), transcriptional regulation (Ma et al., 2002; Postel, 2003), and protein binding interactions (Salerno et al., 2003).

Finally, it has been reported that NM23/NDPK families play an important role not only in tumor metastasis but also in cell growth, differentiation, development and apoptosis (Lombardi et al., 2000). However, despite extensive studies, the whole picture of NM23 relating to its multiple functions is still under way. Our lab focuses on the study of the anti-metastatic mechanisms of NM23-H1.

1.3. Enzymatic Activities and the Potential Anti-metastatic Mechanism(s) of NM23

NM23 proteins have been identified to possess multiple enzymatic activities, but the biological and biochemical mechanism(s) underlying its

ability to suppress metastasis still remain under active investigation. Figure 2 summarizes the primary biochemical activities of NM23-H1 as understood at present, and highlights potential anti-metastatic functions for each.

Figure 2. Potential anti-metastatic functions of the primary enzymatic activities of NM23-H1.
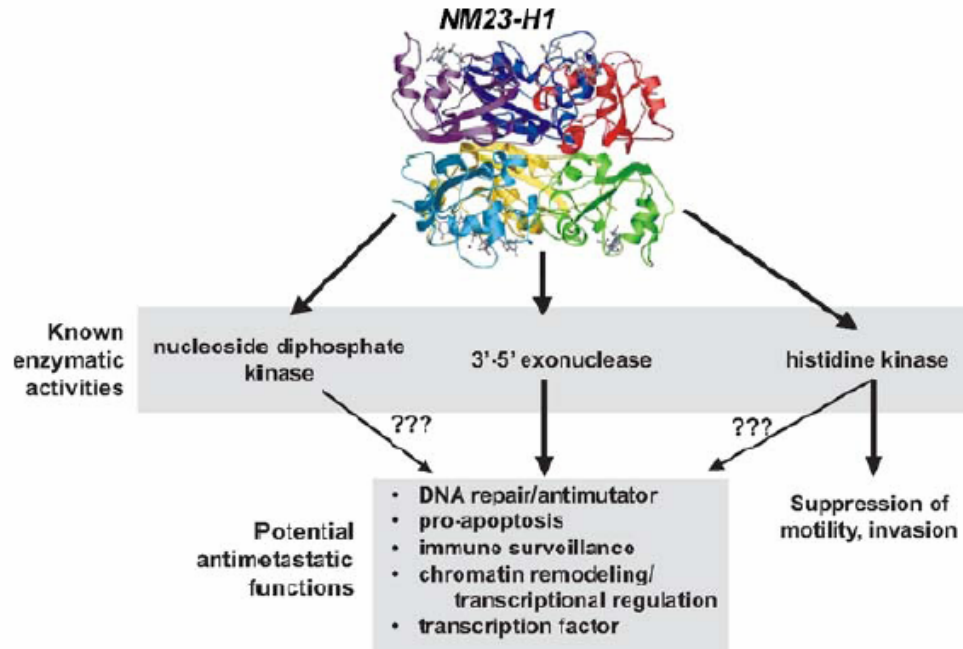
Picture from *2006 J. Bioenerg. Biomembr.* **38**:163 -167

1.3.1. Nucleoside diphosphate kinase (NDPK) activity

NM23 proteins have been characterized as nucleoside diphosphate kinases (NDPK) (Lascu et al., 2000), although not all members in the NM23 family exhibited NDPK activity (in human, only recombinant H1, H2 and H4 contained NDPK activity; (Yoon et al., 2005)). NDPK is a ubiquitous enzyme highly conserved from bacteria to human, which catalyzes the phosphorylation of nucleoside diphosphates to nucleoside triphosphates using ATP as phosphor-donor via a "ping-pong" mechanism (Agarwal et al., 1978). The ping-pong mechanism involves a conserved histidine as the intermediate where the imidazole side chain gets auto-phosphorylated.
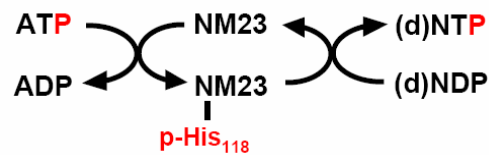
In addition, NDPK is a highly efficient enzyme with a turnover number of about 10^3 s^{-1} and a k_{cat}/K_m of about 10^7 M^{-1} s^{-1}, and utilizes either purine or pyrimidine ribo- or deoxyribonucleosides as substrates (Postel, 1998). As highly efficient phospho-transferases, NDPKs maintain an intracellular nucleotide balance for nucleic acid synthesis and other metabolic functions. However, the gene encoding NDPK is not essential for viability in *E. coli* and yeast (Fukuchi et al., 1993; Lu et al., 1995). Mutants of *E. coli* lacking *ndk* exhibited normal growth rates but showed a mutator phenotype that was attributed to the absence of NDPK catalytic activity or to an imbalance in cellular nucleotide triphosphates (Lu et al., 1995). Although it was suggested that the NDPK activity of NM23-H1 was not essential for suppressing the metastatic potential (MacDonald et al., 1993), this yet needs to be demonstrated using an *in vivo* forced expression model.

1.3.2. Histidine protein kinase activity

Histidine protein kinases are well described in prokaryotes and lower eukaryotes, where they form the "two-component" signal transduction system.

The prototypical two-component regulator system is comprised of two proteins, a histidine protein kinase (sensor protein), which usually binds to the cell membrane, and a response regulator (effector protein), which is associated with an internal response. The sensor kinase, when activated by a signal, autophosphorylates at a histidine residue using ATP as a phosphor-donor. Then, the phosphorylated sensor kinase transfers the phosphoryl group to a conserved aspartate residue in the response regulator. This phosphorylation modulates the activity of the effector protein to elicit an adaptive response to the stimulus (Calera et al., 1998). Several features distinguish histidine protein kinases: (1) histidine is a high energy bond; (2) phosphohistidine is acid labile, and therefore difficult to detect in conventional gel systems; (3) histidine kinases form a phosphohistidine intermediate, which then transfers the phosphate to the substrate (Ouatas et al., 2003).

The histidine protein kinase activity of NM23 was reported to correlate with motility suppression. When wild-type and site-directed mutant ($P_{96}S$ and $S_{120}G$) *nm23-H1* constructs were transfected into MDA-MB-435 breast carcinoma cells, the $P_{96}S$ mutant (histidine kinase deficient) showed impaired motility suppression (MacDonald et al., 1996). In addition to inhibiting metastasis *in vivo* and motility *in vitro* by overexpression of NM23-H1, a diminished Map kinase activation was also found by Steeg and colleagues (Hartsough et al., 2002). Kinase suppressor of Ras (KSR), a scaffold protein for the mitogen-activated protein kinase (MAPK) cascade, was co-immunoprecipitated with NM23-H1 from both transfected 293T cells and human MDA-MB-435 breast carcinoma cells. Autophosphorylated recombinant NM23-H1 phosphorylated KSR *in vitro* and serine was determined as the major target by phosphor-amino acid analysis. In the same paper, they also found that Map kinase activation was reduced in an *nm23-H1* transfected MDA-MB-435 cells. Moreover, the *$P_{96}S$-H1* transfectant exhibited relatively high levels of activated Map kinase, suggesting that the histidine protein kinase activity of NM23-H1 was needed for suppression of Map kinase activation. Therefore, it was hypothesized that overexpression of NM23-H1 increased the KSR phosphorylation and inhibited Map kinase activation, which may contribute to the mechanism of metastasis suppression (Hartsough et al., 2002). However, the relevant downstream substrate of the

histidine kinase and their relationships to metastasis suppression awaits more detailed characterization.

1.3.3. DNA binding and transcriptional regulation

NM23-H2 is recognized as the transcription factor PuF, which activates transcription of the *c-myc* gene *in vitro* by binding to and activating a nuclease-hypersensitive element (NHE) in the c-*myc* promoter (Berberich and Postel, 1995). These *in vitro* findings have been confirmed in living cells (e.g., Burkitt lymphoma cells) by cell transfection assays (Ji et al., 1995). The NHE contains an asymmetric pattern of repeated sequences, "GC" rich regions, which would form unusual structures, including "slipped DNA", loops, triplexes, and G-quadruplex structures (Postel, 2003). In addition, NM23-H2/PuF is capable of recognizing and interacting with such unusual structural elements to activate the *c-myc* gene (Postel, 1998, 1999).

Later, NM23-H1 was identified as a DNA-binding protein to the platelet-derived growth factor-A (*PDGF-A)* chain promoter in our laboratory (Ma et al., 2002). The *PDGF-A* chain promoter is regulated by several enhancer and silencer elements, which are GC-rich and possess non-B DNA structures. NM23-H1 was identified to bind and mediate a silencer element in the 5'-flanking sequence of the *PDGF-A* gene termed 5'-SHS by screening a HeLa cell cDNA expression library with the DNA recognition site approach. Transient transfection analyses in HepG2 cells revealed that both H1 and H2 repressed transcriptional activity driven by the *PDGF-A* basal promoter (-82 to +8), another NHE element. Activity of the negative regulatory region (-1853 to -883), which contained the 5'-SHS, was also inhibited by H1 and H2. These studies demonstrated for the first time that NM23-H1 also interacted with DNA structurally and functionally. They also indicated a role for both NM23 proteins in repressing transcription of an oncogene, providing a possible molecular mechanism to explain their metastasis-suppressing effects.

1.3.4. DNA cleavage activity

NM23-H2 cleaved both DNA strands of a duplex oligonucleotide substrate comprised of the *c-myc* nuclease hypersensitive element (NHE), leaving double-stranded breaks within the repeated sequence elements (Postel, 1999). The breaks produced staggered ends with 5-nucleotide-long 3'-extensions. A covalent protein-DNA complex was suggested between the cleaved 5'-phosphoryl ends and lysine-12 (Postel, 1999). Since covalent protein-DNA complexes were known to serve the roles of breaking and rejoining DNA strands, it was concluded that NM23-H2 was involved in DNA structural transactions necessary for the activity of the *c-myc* promoter (Postel, 2003). Lysine-12 was identified to be the amino acid responsible for the covalent cleavage by NM23-H2 (Postel et al., 2000). In particular, the ε-amino group acted as the critical nucleophile, because substitution with glutamine but not arginine completely abrogated covalent adduct formation and DNA cleavage, whereas the DNA-binding properties remained intact (Postel et al., 2000). These findings and chemical modification data suggested that phosphodiester-bond cleavage by NM23-H2 occurred via a DNA glycosylase/lyase-like mechanism (Postel et al., 2000), which was known as the signature of nucleases in base excision repair (Cunningham, 1997; McCullough et al., 1999). A DNA repair-like activity for NM23 would be consistent with its role in suppressing the metastatic progression.

We focused our attention on the DNA cleavage activity of NM23-H1, in which we demonstrated 3'-5' exonuclease activity by virtue of its ability in stoichiometric amounts to excise single nucleotides in a stepwise manner from the 3' terminus of DNA (Ma et al., 2004). The lines of evidence to support that the 3'-5' exonuclease activity is an intrinsic ability of NM23-H1 are: 1) precise coelution of enzymatic activity with NM23-H1 protein during purification by hydroxylapatite and gel filtration column high performance liquid chromatography and 2) site-specific mutation of a residue shown previously to inactivate the NM23-H2 isoform ($K_{12}Q$) also resulted in a reproducible loss of 3'-5' exonuclease activity in NM23-H1. The DNA-binding and 3'-5' exonuclease activity of NM23-H1 was further confirmed by

mutagenesis assays and NMR studies by the Pfeifer group (Yoon et al., 2005). Generally, 3'-5' exonucleases play critical roles in maintaining genomic stability, and their loss often leads to increased mutation rates. Plus, anti-mutator functions are commonly associated with tumor suppressors. Therefore, this raises the questions: does the 3'-5' exonuclease activity of NM23-H1 play a role in maintaining the genomic integrity of a cell? If so, does this anti-mutator function mediate the metastasis suppressor activity of NM23-H1? These important questions will be addressed in this project.

1.4. Project Objectives

The 3'-5' exonuclease activity is very intriguing in light of the association of these enzymes with DNA repair processes, and the mutator phenotypes often arise as a consequence of their deficiencies (Shevelev and Hubscher, 2002). Progression to the metastatic phenotype is well-recognized to require the accumulation of mutations that permit tumor cells to overcome numerous barriers to metastatic growth. Currently, we propose that the 3'-5' exonuclease activity of NM23-H1 plays an important role in maintaining genomic stability and in turn suppressing metastatic progression of tumor cells. This could be a logical candidate explanation for the anti-metastatic mechanism of NM23-H1.

To test our hypothesis, we used site-directed mutagenesis to generate a panel of NM23-H1 mutants in which the primary biochemical activities of the molecule (NDPK, histidine kinase and 3'-5' exonuclease) have been individually inactivated. The metastasis suppressor activities of these variant NM23-H1 mutants were further analyzed by *in vivo* metastasis assays, in hopes of showing that loss of anti-metastatic function would be related to the inactivated biochemical activity of NM23-H1 mutant. Moreover, in an effort to quantify the contribution of NM23-H1 to its potential anti-mutator function, we initiated experiments in the yeast *Saccharomyces cerevisiae*. *S. cerevisiae* provides an excellent eukaryotic model for rapid and convenient analysis of mutation rates. The budding yeast genome has been sequenced and knockout strains are available for essentially all genes. To measure the extent

to which expression of *YNK1* (NM23 homologue in *S. cerevisiae*) is required for genomic integrity in a cell, mutation rates in *ynk1Δ* strain were measured under basal conditions and genotoxic stress.

The overall goal of this project is to understand the physiological role of the 3'-5' exonuclease activity of NM23-H1, as well as its potential relationship to metastasis suppressor activity.

CHAPTER TWO
SITE-DIRECTED MUTAGENESIS IDENTIFIES RESIDUES NECESSARY FOR MUTIPLE ENZYMATIC ACTIVITIES OF THE METASTASIS SUPPRESSOR, NM23

2.1. Introduction

nm23-H1 was the first identified metastasis suppressor gene on the basis of its reduced expression in highly metastatic melanoma and breast carcinoma cells, and an ability of forced NM23-H1 expression to inhibit metastatic potential without significant impact on the transformed phenotype (Steeg et al., 1988). The human NM23 proteins are composed of six identical subunits of 17-19 kDa each and assemble into hexamers as arrangement of "dimer of trimers". In x-ray crystal structure, as shown in Figure 3B, each monomer folds into four-stranded anti-parallel β sheets surrounded by α helices (Morera et al., 1995; Webb et al., 1995).

NM23-H1 has been discovered to exhibit multiple enzymatic activities, but the mechanism(s) underlying its ability to suppress metastasis still remain controversial. First, the NDP kinase activity of NM23-H1 plays an important role in maintaining nucleotides balance; however, its relevance to metastasis suppression is still uncertain. Second, the histidine kinase activity of NM23-H1 was reported to correlate with motility suppression. NM23-H1 mutants (e.g. $P_{96}S$ and $S_{120}G$) exhibited a decreased activity in histidine-dependent protein phosphotransferase *in vitro* (Freije et al., 1997). Both mutants lacked the motility-suppressing capacity of the wild-type NM23-H1 when overexpressed in MDA-MB-435 breast carcinoma cells (MacDonald et al., 1996). However, the *in vivo* downstream substrate of the histidine kinase activity of NM23 is still not clear. The relevance of this activity to metastasis suppression needs to be examined in an animal model. Finally, NM23-H2 was able to cleave the internal sites within the nuclease-hypersensitive element (NHE) sequence (Postel, 1999), which was further characterized as DNA glycosylase/lyase-like mechanism, a hallmark of base excision DNA repair enzymes (Postel et al., 2000). Moreover, our laboratory has recently identified that recombinant NM23-H1 possesses significant 3'-5' exonuclease activity *in vitro* (Ma et al.,

2004). Generally, enzymes that contain 3'-5' exonuclease activity are involved directly in DNA repair processes and maintenance of genomic stability (Shevelev and Hubscher, 2002). Therefore, we hypothesized that loss of the 3'-5' exonuclease activity of NM23-H1 during tumor progression could possibly impair genomic integrity and increase mutation rates, thereby enhancing the metastatic potential. However, due to the multiple impacts of metastasis suppressor on a cell, contributions from other biochemical pathway to metastasis suppression also need to be considered.

To study the active sites for the multiple enzymatic activities of NM23-H1, site-directed mutagenesis was initiated in our laboratory. Previous studies in our laboratory identified amino acid residues important for the enzymatic characteristics of NM23-H1. For instance, lysine$_{12}$ was necessary for both the cleavage and NDP kinase activities of NM23-H1; whereas histidine$_{118}$, the NDPK catalytic site, to phenylalalnine mutation led to a total loss of NDP kinase activity (Ma et al., 2004). However, none were selective for disrupting the exonuclease activity. To test our hypothesis that the 3'-5' exonuclease activity of NM23-H1 might mediate its suppressing effects on metastasis, the first goal was to identify a mutant selectively disrupted in the 3'-5' exonuclease activity. Therefore, more amino acid residues were targeted to be substituted. First, the substitution of glutamine$_{17}$ to asparagine ($Q_{17}N$) of NM23-H2 identified that the necessity of residue Gln$_{17}$ was only for DNA cleavage but not NDP kinase activity (Postel et al., 2002). Since 88% of the amino acid residues in the NM23-H1 protein are identical to NM23-H2, the similar results were expected to be exhibited in NM23-H1 based on the same residue substitutions. Second, the residue Glu$_5$ was recently reported to be critical for DNA cleavage activity of NM23-H1 (Yoon et al., 2005). To fully understand the importance of this residue on the multiple enzymatic activities of NM23-H1, a Glu$_5$ to alanine mutation (E_5A) was introduced as part of this study. Third, our laboratory found the residues Tyr$_{52}$ and Asp$_{54}$ of NM23-H1 are homologous with the same residues on the EXOIII domain of known 3'-5' exonucleases. The EXOIII motif has been identified as the required DNA cleavage domain, which was highly conserved in selected 3'-5' exonucleases from prokaryotic to mammalian species (Shevelev and Hubscher, 2002). Therefore, these two residues were believed to be important for the

15

exonuclease activity of NM23-H1 and needed to be tested. Finally, a Pro$_{96}$ to serine (P$_{96}$S) substitution was included due to its importance on histidine kinase activity of NM23-H1 (Freije et al., 1997). The relevance of this residue on the DNA cleavage activity needed to be further examined. Taken together, the complete generation of variant NM23-H1 mutants would provide a useful foundation to study the anti-metastatic function of the molecule.

Figure 3. The structure of NM23-H1 (A) Amino acid sequence and schematic representation of NM23-H1 indicating major secondary structural features, the α helices, β sheets and Kpn loop. The substituted amino acids are labeled in bold font. (B) Ribbon diagram of an NM23-H1 monomer, folding as four-stranded anti-parallel β sheets surrounded by α helices. (C) Space-filling model of the NM23-H1 hexamer. Side chains of the substituted amino acid residues are labeled as indicated.

A.

| β 1 | α 0 | α 1 | β 2 | α A | α 2 | β 3 |

```
         5        10      15       20       25      30        35      40        45      50       55      60        65      70        75      80
MANCERTFIAIKPDGVQRGLVGEIIKRFEQKGFRLVGLKFMQASEDLLKEHYVDLKDRPFFAGLVKYMHSGPVVAMVWEG
```

| α 3 | Kpn loop | β 4 | α 4 |

```
      85       90       95      100     105      110      115     120      125     130      135     140      145     150
LNVVKTGRVMLGETNPADSKPGTIRGDFCIQVGRNIIHGSDSVESAEKEIGLWFHPEELVDYTSCAQNWIYE
```

B.

17
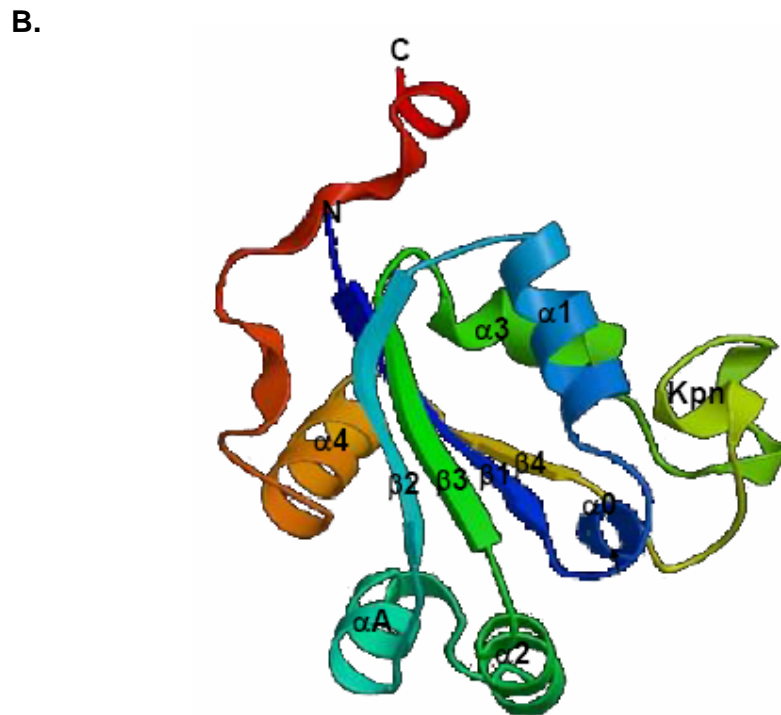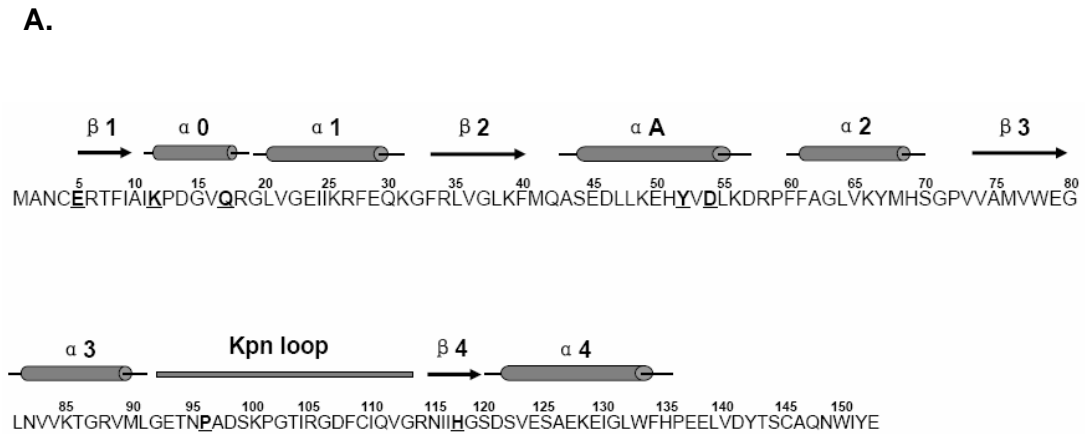
C.
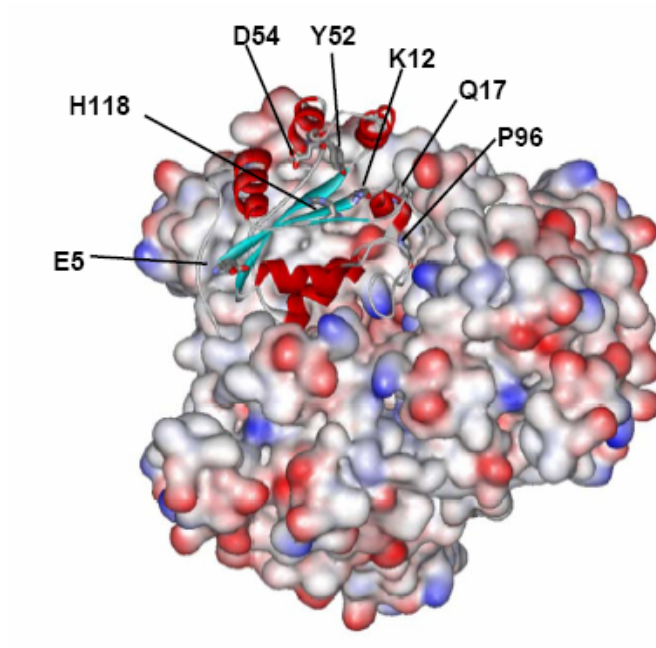
2.2. Materials and Methods

2.2.1. DNA and site-directed mtagenesis

cDNAs encoding the NM23-H1 mutant variants $Q_{17}N$, $Y_{52}A$, $D_{54}A$ and $P_{96}S$ were generated by the overlap extension modification of the polymerase chain reaction (PCR), as described (Ho et al., 1989), and were inserted in frame between the NdeI and BamHI sites of the *E. coli* expression plasmid pET3c (New England Biolabs). The E_5A mutant was constructed using the QuikChange site-directed mutagenesis kit (Stratagene). The mutagenic primers to construct the E_5A, $Q_{17}N$, $Y_{52}A$, $D_{54}A$ and $P_{96}S$ mutants are shown in Table 1 (codons encoding the mutant residue are underlined in bold font). The cloned PCR products were sequenced by ACGT and Elim Biopharmaceutical Inc. to ensure that only the desired mutation was present. pET3c plasmids containing wild-type NM23-H1 and the $H_{118}F$ mutant were kindly provided by E. Postel (Princeton University), while construction of $K_{12}Q$ was described previously (Ma et al., 2004).

Table 1. The mutagenic primers to construct the E_5A, $Q_{17}N$, $Y_{52}A$, $D_{54}A$ and $P_{96}S$ mutants. Codons encoding the mutant residue are underlined in bold font.

NM23-H1 mutation	Forward mutagenic primer 5'→3'	Reward mutagenic primer 5'→3'
E_5A	ATG GCC AAC TGT **GCT** CGT ACC TTC	GAA GGT ACG **AGC** ACA GTT GGC CAT
$Q_{17}N$	CCA GAT GGG GTC **AAC** CGG GGT CTT	AAG ACC CCG **GTT** GAC CCC ATC TGG
$Y_{52}A$	AAG GAA CAC **GCC** GTT GAC CTG AAG G	C CTT CAG GTC AAC **GGC** GTG TTC CTT
$D_{54}A$	GAA CAC TAC GTT **GCC** CTG AAG GAC CG	CG GTC CTT CAG **GGC** AAC GTA GTG TTC
$P_{96}S$	GAG ACC AAC **TCA** GCA GAC TCC	GGA GTC TGC **TGA** GTT GGT CTC

2.2.2. Overexpression and purification of recombinant human NM23-H1 and NM23-H2 proteins

NM23-H1 and mutant proteins were expressed and purified by our standard protocol as previously described (Ma et al., 2004; Ma et al., 2002). Briefly, pET3c vectors containing wild-type and variants of NM23-H1 were used to transform *E. coli* (BL21 p*lys*S; Promega). For protein expression, freshly transformed bacteria were grown overnight at 37 °C in LB-ampicillin medium. Two ml of the overnight culture was used to inoculate 200 ml of LB medium containing ampicillin. When A600 reached 0.6, protein expression was induced by the addition of isopropyl-1-thio-β-D-galactopyranoside (final concentration of 0.4 mM). Three hours following the induction, cells were harvested, resuspended in 30 ml of lysis buffer (50 mM Tris, pH 8.0) containing 1 mM EDTA and dithiothreitol, 1 mM leupeptin and pepstatin A, and 0.1 mM phenylmethylsulfonyl fluoride (Sigma), and then lysed by sonication. Cell lysates were cleared by centrifugation at 12,000 x *g* for 30 min and proteins were precipitated with ammonium sulfate (60-90% fractions). The 60-90% fraction was prepared for application to a DEAE-Sephacel column by dialysis into 50 mM Tris buffer (pH 7.5) containing a mixture of protease inhibitors. Next, NM23-H1 bound to the column was eluted with a 0–1 M NaCl gradient and peak fractions at ~350 mM NaCl were collected. Peak fractions containing NM23 proteins were equilibrated in 10 mM phosphate buffer (pH 7.0) by centrifugal filtration (Centricon-10, Millipore) and loaded onto a hydroxyapatite (HTP) column. NM23-H1 was eluted with an 80-ml phosphate gradient of 10-800 mM (pH 7.0). Purity of recombinant proteins was evaluated by SDS-PAGE and Commassie Blue and/or silver staining. NM23-H2 proteins were expressed and purified by the same procedure as NM23-H1 except that NM23-H2 plasmids were transformed into *E. coli* BL21 strain (Promega), not BL21 p*lys*S.

2.2.3. 3'-5' exonuclease assay

The reactions were performed as described (Ma et al., 2002) with a single-stranded, 33-base oligodeoxyribonucleotide substrate corresponding to

the noncoding strand of the 5'-SHS silencer element (5'-SHS antisense strand, or 5'-SHSas) from the platelet-derived growth factor A gene (Liu et al., 1996). 5'-termini were radio-labeled in a 40-μl reaction mixture at 37 °C for 30 min using [γ-^{32}P]ATP and T4 polynucleotide kinase. DNA cleavage reactions were conducted at ambient room temperature in a 15-μl volume containing 20 mM Hepes buffer (pH 7.9), 10-20 fmol of 5'-[^{32}P]-labeled oligonucleotide, 2 mM MgCl$_2$ and 100 mM KCl, and were initiated by the addition of 1 μg NM23-H1 (640nM). Reactions were terminated by adding an equal volume of sequencing loading dye consisting of 80% deionized formamide (w/v), 10 mM EDTA (pH 8.0), xylene cyanol FF (1 mg/ml), and bromphenol blue (1 mg/ml) followed by heating at 95 °C for 5 min. Cleavage products were resolved on 14% sequencing gels and visualized by phosphoimaging (Storm 860, Amersham Biosciences).

.2.2.4. Nucleoside-diphosphate kinase assay

NDPK activity of NM23-H1 and variant mutants was measured as described (Agarwal et al., 1978) by a coupled pyruvate-lactate dehydrogenase assay in which ATP acted as a phosphate donor and dTDP as an acceptor. The procedure was modified for the use of 96-well plates and microplate reader (Ma et al., 2004). NDPK reactions were initiated by the addition of 10 μl of purified NM23-H1 (10-50 ng) to a 140-μl reaction mixture containing 1 mM pyruvate enol phosphate, 5 mM ATP, 2.5 mM dTDP, 6 mM MgCl$_2$, 50 mM KCl, 1000 units of pyruvate kinase and lactate dehydrogenase in 100 mM Tris-HCl, pH 7.4. NAD$^+$ formation, which reflected ADP production, was measured every 25 seconds at 340 nm by a HTS 7000 plus Bioassay Plate Reader (PerkinElmer). Specific activity was expressed as units/mg of protein, with 1 unit defined as the amount of enzyme converting 1 μmol of ADP/min at room temperature (ε_{340} of NADH = 6.22 x 10^3 M^{-1} cm^{-1}).

2.2.5. Circular dichroism analysis

Far UV-CD spectra were recorded from 260 to 190 nm using a Jasco J-810 spectrometer, with each individual spectrum representing the average of

30 replicate measurements. Prior to analysis, purified NM23-H1 proteins were diluted to a concentration of 0.12 mg/ml in 5 mM phosphate buffer (pH 7.0) (ε_{280} = 1.35 for a 1 mg/ml solution; (Lascu et al., 1997)). CD spectra were recorded at 5 °C in a quartz cuvette with a 0.1-cm path-length. CD data were converted to mean residual ellipticity, assuming a hexameric structure and mean residue molecular mass of 113 Da, the latter calculated from a 152-amino acid monomer with a molecular mass of 17,180 Da (Rosengard et al., 1989). Secondary structure estimates were derived from the 250–190 nm region of the recorded CD spectra using the programs CONTILL, SELCON3, and CDSSTR and their reference set of 43 proteins (Sreerama and Woody, 2000) from CDPro software package (lamar.colostate/edu~sreeram/CDPro/).

2.2.6. High performance liquid chromatography (HPLC) gel filtration

Purified wild-type or mutant variants of NM23-H1 were analyzed as described (Ma et al., 2004). Briefly, proteins were loaded on a Shodex gel filtration HPLC column (Shodex Protein KW-800, Showa Denko) pre-equilibrated in 50 mM Tris-HCl (pH 7.5), 0.1 M KCl. Molecular weights of NM23-H1 were estimated relative to a standard curve generated with a commercially available molecular mass standards kit (Sigma) containing cytochrome C (12.4 kDa), carbonic anhydrase (29 kDa), bovine serum albumin (66 kDa), alcohol dehydrogenase (150 kDa), β-amylase (200 kDa), and blue dextran (2,000 kDa).

2.3. Results

2.3.1. DNA sequencing verified only the desired mutations present

The site of the substituted amino acids in the sequence of NM23-H1 is indicated in Figure 3, panel A and C. The cloned PCR products were sequenced by sense and anti-sense strands to ensure that only the desired mutation was present (Figure 4).

Figure 4. Sequence verification of PCR-generated cDNAs of NM23-H1 mutants. Double strands of cloned NM23-H1 DNA were sequenced to verify that only the desired substitution was present. The substituted nucleotides were underlined in the histogram profile. (A) E_5A-H1 (B) $Q_{17}N$-H1 (C) $Y_{52}A$-H1 (D) $D_{54}A$-H1 (E) $P_{96}S$-H1

A.   E(gag)→A(gct)

B.   Q(cag)→N(aac)

C.   **Y(tac)➔A(gcc)**

$Y_{52}A$ substitution

Sense-strand   Antisense-strand

D.   **D(gac)➔A(gcc)**

$D_{54}A$ substitution

Sense-strand   Antisense-strand

E.   **P(cct)➔S(tca)**

$P_{96}S$ substitution

Sense-strand   Antisense-strand

25
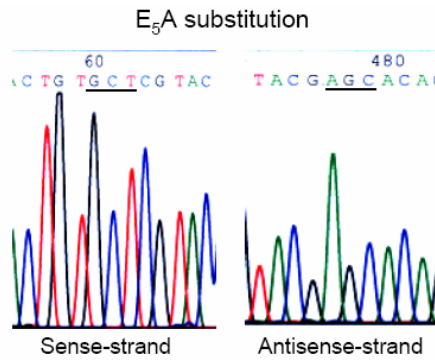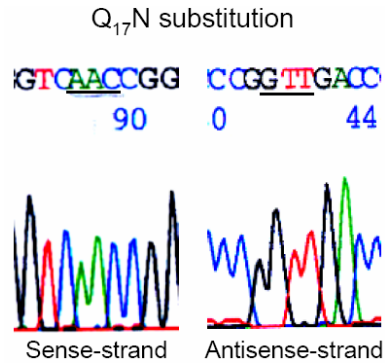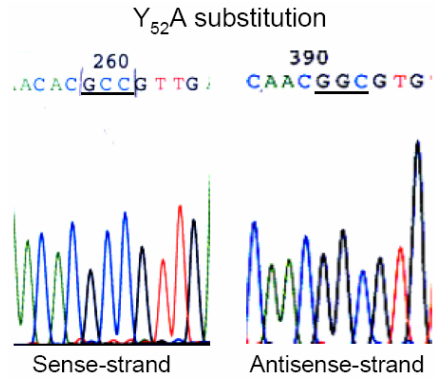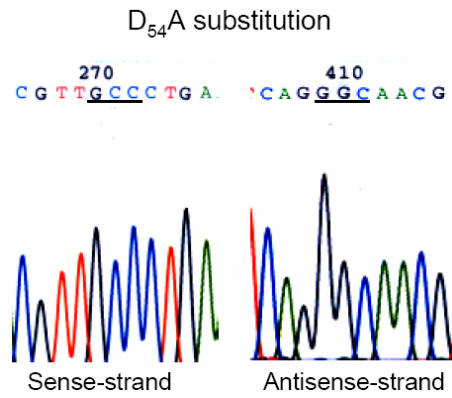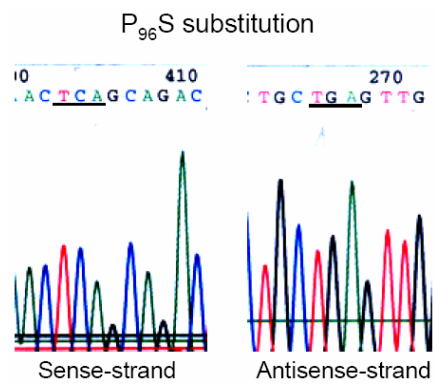
2.3.2. Recombinant NM23-H1 and NM23-H2 proteins were overexpressed and purified

NM23-H1 variants were purified with a three-step protocol consisting of ammonium sulfate precipitation and sequential chromatographic steps of DEAE-Sephacel and hydroxylapatite. Compared to the elution time of wild-type NM23-H1 (82-83 min, Figure 5, panel A) from the hydroxylapatite column, the $P_{96}S$ mutant (Figure 5, panel E) was eluted slightly earlier (81-82 min); the $Y_{52}A$ mutant (Figure 5, panel D) was eluted much earlier (69-70 min); the E_5A mutant (Figure 5, panel B) was eluted slightly later (84-85 min); while The $Q_{17}N$ was eluted at the same position of the phosphate gradient as the wild-type protein (Figure 5, panel C, 82-83 min),

Figure 5. Hydroxylapatite column chromatography of wild-type and mutant NM23-H1. Figures shown below are elution profiles from the final step of purification involving HTP column chromatography. HTP chromatography was conducted using a Waters HPLC system at a flow rate of 1 ml/min, with NM23-H1 proteins eluted using an 80-ml gradient of potassium phosphate (10–800 mM, pH 7.0) and the collection of 1-min fractions. Within each of panels A–E, A280 profile (top) and analysis of column fractions by SDS-PAGE gel with Coomassie staining (bottom) are shown. The elution time of the NM23-H1 variants from the HTP column are (A) 82-83 min for wild-type H1. (B) 84-85 min for E_5A-H1. (C) 82-83 min for $Q_{17}N$-H1. (D) 69-70 min for $Y_{52}A$-H1. (E) 81-82 min for $P_{96}S$-H1.

A.
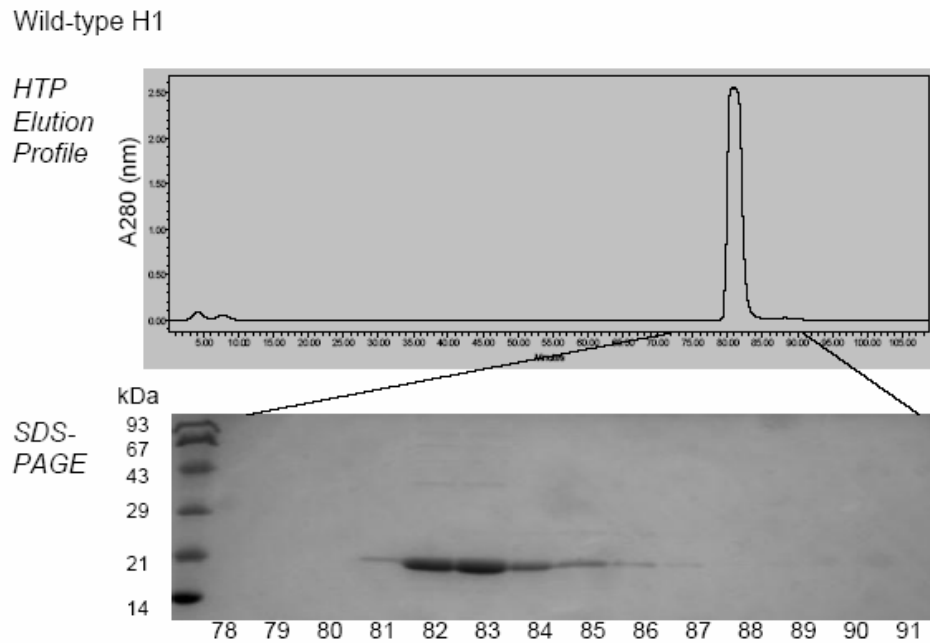
B.

E$_5$A-H1

C.

Q$_{17}$N-H1

28

D.

Y$_{52}$A-H1

HTP Elution Profile
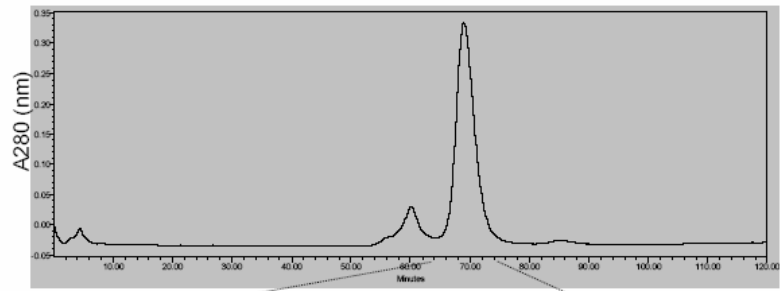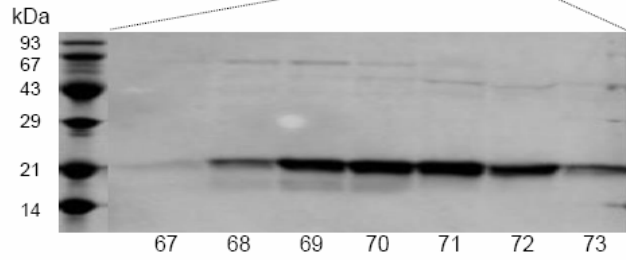
SDS-PAGE Gel

E.

P$_{96}$S-H1

HTP Elution Profile
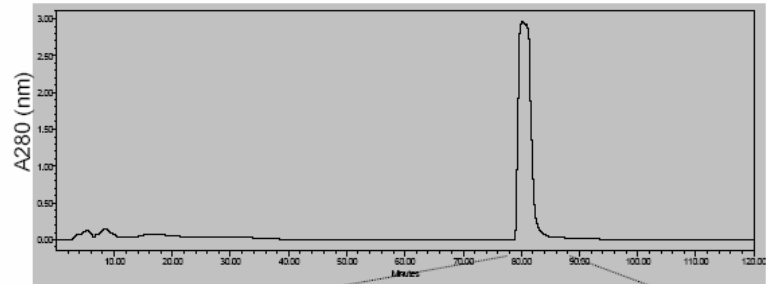
SDS-PAGE Gel
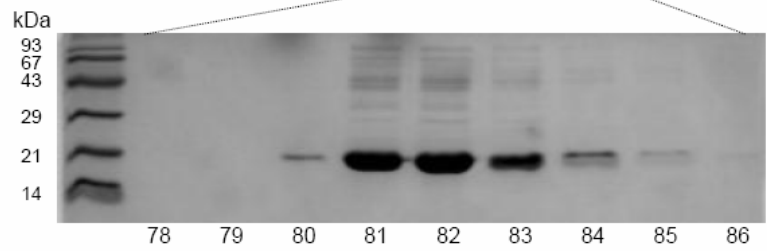
2.3.3. 3'-5' Exonuclease activity of NM23-H1 mutants was measured

To assess the effects of these amino acid substitutions on DNA cleavage activity, 1 µg of wild-type or mutant NM23-H1 protein was incubated with 10–20 fmol of 5'-[^{32}P]-labeled 5'-SHSas oligodeoxyribonucleotide at 22 °C during a 1-hour time course (5, 10, 15, 20, 40, 60min) in the presence of 2 mM MgCl$_2$ and 100 mM KCl. Cleavage products were analyzed by electrophoresis through denaturing 14% polyacrylamide gel and visualized by phosphorimaging. Wild-type NM23-H1 elicited the rapid appearance of products representing progressive removal of single nucleotides from the 3' terminus with increasing incubation time (Figure 6A, lanes 2-7). 60 minutes of incubation yielded substantial DNA fragments ranging between 15 and 17 nt (Figure 6A, lane 7). The Q$_{17}$N and P$_{96}$S mutants produced very similar cleavage activity as the wild-type H1, presenting time-dependent appearance of progressive single nucleotide digestion from 3' terminus to 5' terminus on the single strand DNA substrate (Figure 6A, lanes 8-13 and 14-19, respectively). The Y$_{52}$A mutant generated less digested fragments than the wild-type protein, while still yielding a considerable quantity of the 15–33-nt series of fragments (Figure 6A, lanes 20-25). Digestion by the E$_5$A mutant are significantly reduced, evidenced by much slower rate of depletion of the full-length substrate (Figure 6A, lanes 26-31). The results of cleavage activity of the E$_5$A, Q$_{17}$N, Y$_{52}$A and P$_{96}$S mutants were consistently seen with three or more replicate preparations of each protein. The diminished 3'-5' exonuclease activity of the E$_5$A mutant indicated a potential role for Glu$_5$ in the catalytic mechanism. Therefore, besides Lys$_{12}$, a critical site of DNA cleavage activity as previous reported (Ma et al., 2004), Glu$_5$ is another amino acid residue important for 3'-5' exonuclease activity of NM23-H1.

Figure 6. 3'-5' exonuclease activity of purified NM23-H1 mutants. A, 1 μg of wild-type (WT) or mutant ($Q_{17}N$, $P_{96}S$, $Y_{52}A$, E_5A) NM23-H1 protein was incubated with 10 fmol of ^{32}P-labeled 5'-SHS-AS oligodeoxynucleotide under standard cleavage assay conditions during the indicated time. B, Cleaved products were quantified by phosphorimaging to derive the cleaved amount of nucleotides.

A.

B.

31
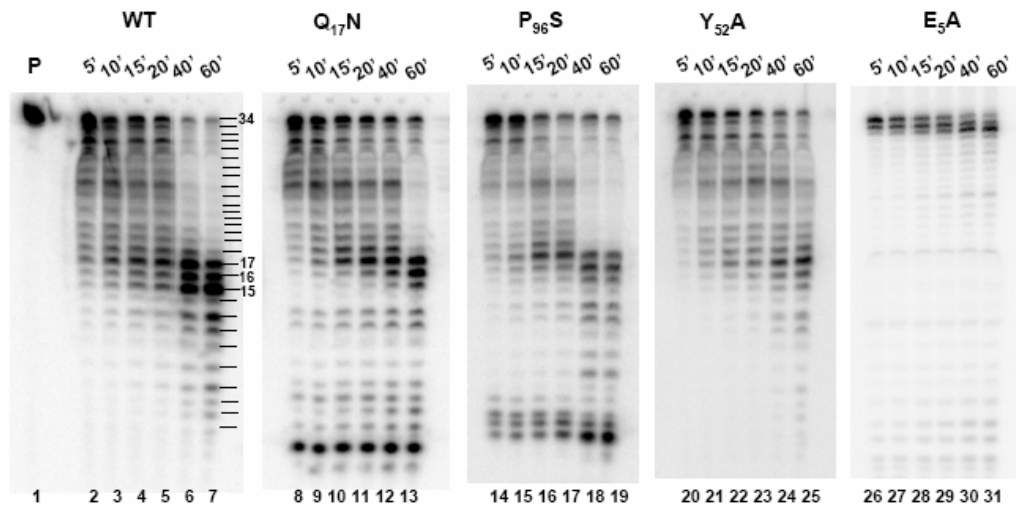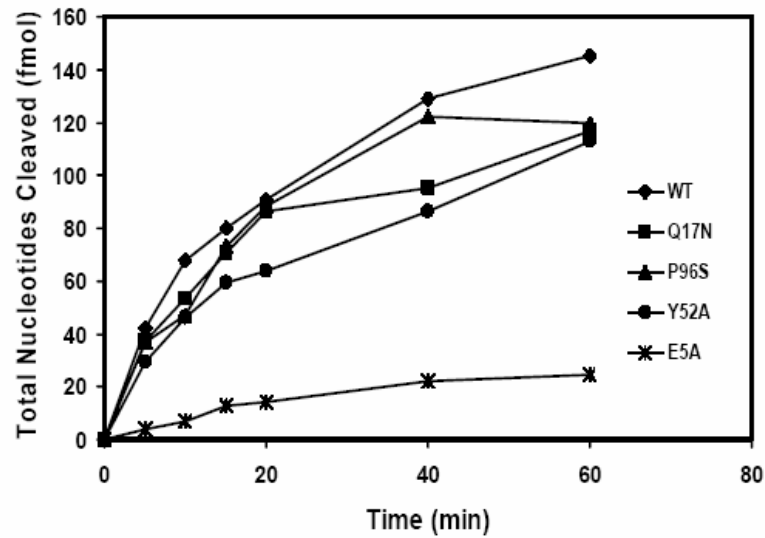
2.3.4. NDPK activity of NM23-H1 mutants was measured

NDPK activity was measured using a coupled pyruvate kinase/lactate dehydrogenase assay as described previously (Agarwal et al., 1978; Ma et al., 2004). The average specific NDPK activity of wild-type NM23-H1 was 630 units/mg. Compared to this, the E_5A and $Q_{17}N$ mutants retained 70-80% NDPK activity of the wild-type (440 units/mg and 520 units/mg, respectively, Table 2), consistent with the effect of $Q_{17}N$-H2 mutant on this kinase activity (Postel et al., 2002). The NDPK activity of the $P_{96}S$ mutant was 127 units/mg (Table 2), not consistent with a previous report, in which it was shown the $P_{96}S$-H1 mutant retained full NDPK activity (Freije et al., 1997). However, this inconsistency is not surprising, because the Freije group used a different method from the one we used. They determined the formation of $[\gamma-^{32}P]GTP$ from non-radioactive GDP when incubated with $[\gamma-^{32}P]ATP$ and NM23-H1. However, the method we used was to quantify the specific activity of the enzyme, which was more accurate and reliable. Finally, the NDPK activity of $Y_{52}A$ mutant was dramatically inhibited (below the detection limits; Table 2), indicating Y_{52} was likely to play a critical role in the NDPK activity of NM23-H1.

Table 2. NDPK, histidine kinase and 3'-5' exonuclease activities for NM23-H1 variants.

Protein	NDPK		Histidine Kinase		3'-5' Exonuclease	
	activity[1]	% of WT	activity[2]	% of WT	activity[3]	% of WT
WT	627 ± 36^e	100	9.9	100	28.4 ± 4.0	100
E_5A	438 ± 31^d	70	8.2	83	$3.4 \pm 1.5^*$	12
$K_{12}Q$	$14 \pm 0.9^{b,4}$	2	0.9	9	$5.2 \pm 3.5^*$	18
$Q_{17}N$	516 ± 10^d	82	6.5	66	31.4 ± 6.0	110
$Y_{52}A$	B.D.^{a}	0	0.4	4	25.3 ± 3.9	89
$P_{96}S$	127 ± 5^c	20	1.1	11	24.9 ± 5.1	88
$H_{118}F$	B.D.^{a,4}	0	B.D.	0	33.0 ± 9.0	116

[1]NDPK activity is expressed as the mean ± S.E. in units/mg proteins, derived from at least three different protein preparations.

[2]Histidine kinase activity is expressed as a percent of substrate converted per minute. (Assays performed by Robert McCorkle.)

[3]Exonuclease activity is expressed in fmol/5min (mean ± S.E.) and is derived from at least three assays conducted with at least three independent protein preparations.

[4]Values shown for NDPK activity of $K_{12}Q$ and $H_{118}F$ were published previously (Ma et al., 2004).

[a-d] Means not showing a common superscript are significantly different ($p \leq 0.01$).

[*]Means bearing an asterisk within a column are significantly different ($p \leq 0.05$).

B.D., below detection.

2.3.5. Oligomeric structure of NM23-H1 mutants was not significantly changed based on molecular weight estimates

The purified mutant NM23-H1 variant proteins were further analyzed by gel filtration HPLC to estimate oligomeric structure and molecular weight. Two peaks were observed with wild-type NM23-H1 protein (Figure 7), a primary peak at approximately 18.74 min with an estimated molecular mass of 87.7 kDa (Table 3) and a minor peak at about 17.1 min. Our previous evidence showed that the DNA cleavage activity precisely coeluted with the primary peak of oligomerized NM23-H1 protein (Ma et al., 2004), suggesting the minor peak could be some nonspecific copurified contaminants. The primary peak of NM23-H1 mutants was observed at 18.78(E_5A), 18.76($Q_{17}N$), 18.90($Y_{52}A$) and 18.79($P_{96}S$) minute, respectively. Molecular weight estimates obtained by gel filtration HPLC for E_5A, $Q_{17}N$ and $P_{96}S$ were not significantly different from that of wild-type NM23-H1 (Table 3). $Y_{52}A$ exhibited a small, but statistically significant decrease (9 kDa) in apparent size. However, this small decrease was not consistent with an effect on oligomeric structure and was possibly due to anomalous interaction of this aromatic-structure-changed variant with the gel filtration matrix. In summary, none of the mutations resulted in significant disruption of oligomeric structure of the NM23-H1 molecule.

Figure 7. Gel filtration HPLC of wild-type and mutant NM23-H1. Purified wild-type or mutant NM23-H1 proteins were loaded on a Shodex gel filtration HPLC column (Shodex Protein KW-800) pre-equilibrated in 50 mM Tris (pH 7.5) and 0.1 M KCl at a flow rate of 0.5 ml/min. Elution times of the molecular mass standards (Sigma) cytochrome *c* (12.4 kDa), carbonic anhydrase (29 kDa), bovine serum albumin (66 kDa), alcohol dehydrogenase (160 kDa), β-amylase (200 kDa), and blue dextran (2000 kDa) are indicated with arrows. The primary peaks of the NM23-H1 variants eluted from the gel filtration column are (A) 18.74 min for wild-type NM23-H1. (B) 18.78 min for E_5A-H1. (C) 18.76 min for $Q_{17}N$-H1. (D) 18.90 min for $Y_{52}A$-H1. (E) 18.79 min for $P_{96}S$-H1.

A.

B.

35
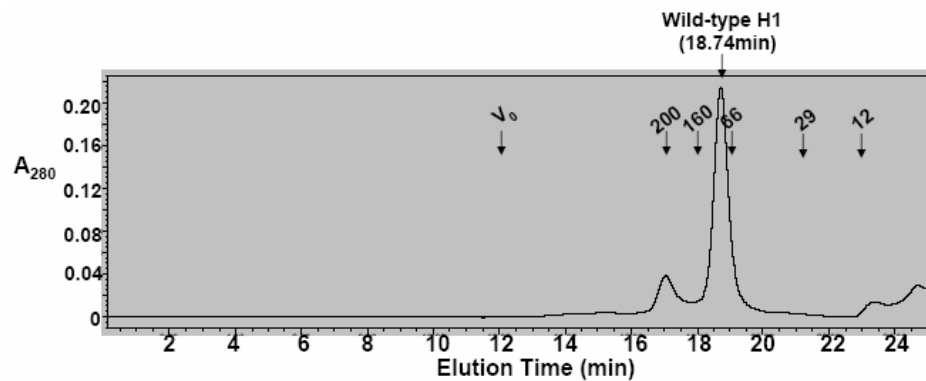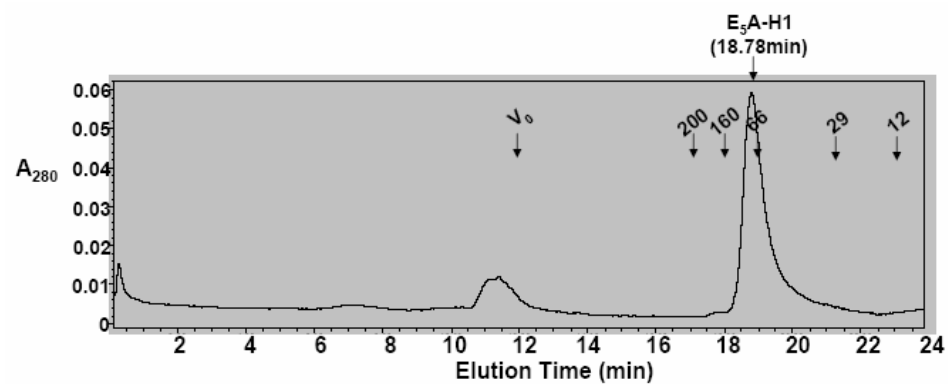
C.
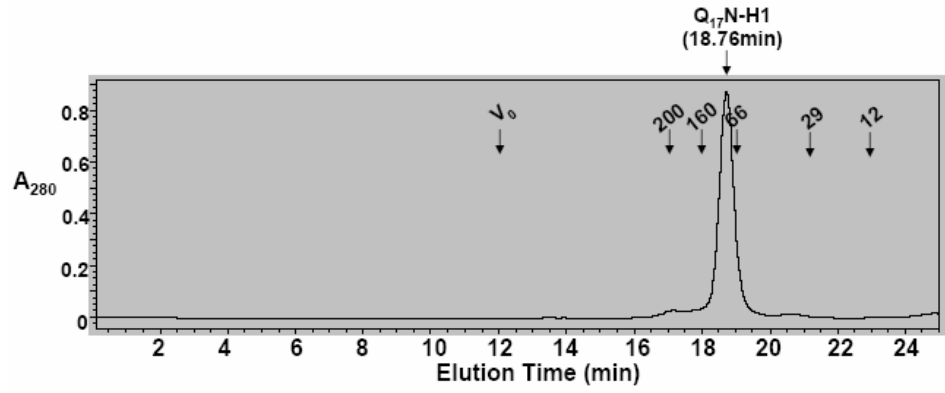
D.
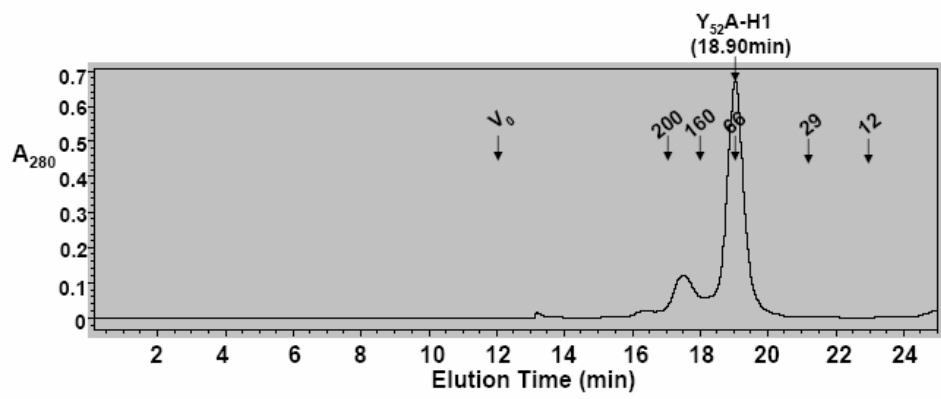
E.
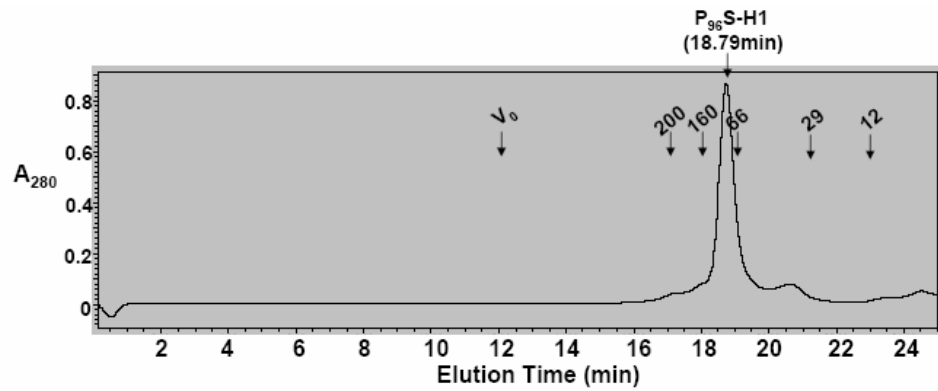
Table 3. Molecular weight estimates of NM23-H1 mutants.

Protein	Estimated Molecular Weight[1]
WT	87.7 ± 2.1
E_5A	85.1 ± 7.1
$Q_{17}N$	86.3 ± 1.5
$Y_{52}A$	78.4[*] ± 3.0
$P_{96}S$	84.7 ± 0.4

[1] Results were obtained by gel filtration HPLC and are expressed as the mean ± S.D. in kDa of three replicate determinations (> 2 independent protein preparations).

[*] Means within a column bearing an asterisk are significantly different ($p<0.05$).

2.3.6. Circular dichroism analysis indicated NM23-H1 mutants exhibited normal secondary structure

To measure the extent to which the mutations affected secondary structure of the NM23-H1 molecule, purified proteins were analyzed by circular dichroism (CD) spectrometry. The CD spectra obtained for the wild-type NM23-H1 (Figure 8) were consistent with the previous report (Ma et al., 2004) using the same procedure. The secondary structure estimates of wild-type NM23-H1 were 14% of total α-helix, 33% of β-sheet, 20% of turns, and 33% of random (Table 4). The CD spectra associated with the E_5A, $Y_{52}A$ and $P_{96}S$ variants were similar to the wild-type, while the $Q_{17}N$ yielded slightly lower helix and higher sheet content than that of wild-type (Table 4). Taken together, the gel filtration and CD spectral analyses indicated that each of the NM23-H1 mutants employed in this study exhibited normal oligomeric and 3-dimensional structure.

Figure 8. Circular dichroism (CD) analysis of recombinant NM23-H1 variants. 1.2 μM of purified wild-type (WT) and mutant NM23-H1 proteins (E_5A, $Q_{17}N$, $Y_{52}A$ and $P_{96}S$) were analyzed by CD spectra at 5 $^{\circ}$C in a 200-μl cuvette (0.1-cm optical path), as described previously (Ma et al., 2004). Each spectrum was the average of 30 measurements and data were expressed as molar ellipticity.
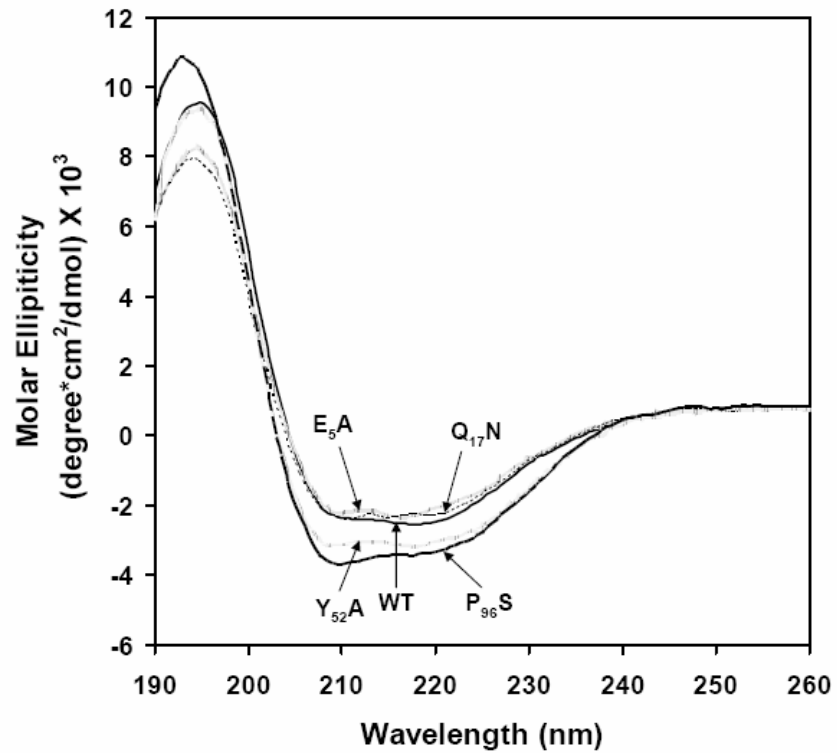
Table 4. Secondary structure estimates of NM23-H1 mutants.

Protein	CD spectrometry[1]			
	α Helix	β Sheet	Turns	Random
WT	14.2 ± 2.8	32.6 ± 5.3	20.0 ± 0.1	32.6 ± 3.8
E_5A	10.7 ± 2.2	35.0 ± 2.5	19.4 ± 0.6	32.9 ± 1.8
$Q_{17}N$	8.8 ± 2.6	40.2 ± 4.3	18.7 ± 2.0	32.3 ± 0.7
$Y_{52}A$	11.4 ± 4.1	35.9 ± 1.9	19.4 ± 1.4	30.7 ± 1.1
$P_{96}S$	13.7 ± 1.7	33.0 ± 1.2	19.8 ± 1.3	32.7 ± 2.0

[1] Secondary structure content is expressed as a percent of the total structure and it represents the mean ± S.D. of estimates provided by the three different structure prediction programs Contin, Selcon3 and CDSSTR from the online DICHROWEB server (lamar.colostate/edu~sreeram/CDPro/).

2.4. Discussion

To assess the relevant roles for each of these biochemical activities of NM23-H1 in metastasis suppression, we created a panel of NM23-H1 variants with selective enzymatic lesions. Previous reports showed that a His$_{118}$→ Phe (H$_{118}$F) substitution totally disrupted NDPK activity but did not affect 3'-5' exonuclease activity, while a K$_{12}$Q mutation disrupted both NDPK and 3'-5' exonuclease activities (Ma et al., 2004). In the current study, we show that the histidine kinase (hisK) activity is also inactivated in each of the aforementioned mutants (H$_{118}$F-0% of WT; K$_{12}$Q-9% of WT; Table 2). Therefore, the K$_{12}$Q mutant harbors profound lesions in all three enzymatic activities (98% reduction in NDPK, 91% loss of hisK, and 82% loss of 3'-5' exonuclease), indicating that Lys$_{12}$ is required for all enzymatic activities associated with NM23-H1. More importantly, E$_5$A substitution results in a dramatic and selective disruption in 3'-5' exonuclease capacity (12% of WT) without significant effect on either NDPK or hisK activity, suggesting that the active site for the kinase and exonuclease activities could be separated. Moreover, loss of the DNA cleavage activity in the E$_5$A and K$_{12}$Q mutants further confirms that the 3'-5' exonuclease activity of NM23-H1 is not due to contamination by bacterial nucleases but is an intrinsic activity of the proteins.

Interestingly, although both of Lys$_{12}$ and Glu$_5$ are necessary for DNA cleavage activity of NM23-H1, their mechanisms of action are not the same. In contrast to lysine acting as a critical nucleophile through the ε-amino group, glutamic acid functions as a nuclease by binding the γ-carboxyl group with divalent cation (Shen et al., 1996). Both of these amino acids are highly conserved in human NM23 homologues from H1 to H5.

Analysis of these mutant proteins by circular dichroism spectrometry revealed that none of the amino acid substitutions resulted in significant alterations in the secondary structure of NM23-H1. Therefore, losses in enzymatic activity observed in this study are likely to reflect specific roles for the respective amino acid residues in enzyme activity.

The enzymatic activities of NM23-H1 demonstrated *in vitro* could have potential implications for such *in vivo* processes as DNA replication and repair. Conversely, loss of these functions would be expected to lead to accelerated

mutation rates, thereby promoting the malignant progression. To test our hypothesis that the 3'-5' exonuclease activity of NM23-H1 may underlie the biochemical mechanism of metastasis suppressor by its potential DNA repair function, the panel of H1 mutants was generated. The enzymatic deficient H1 mutants would permit identifications of the relevant enzymatic activity of NM23-H1. For example, in metastatic tumor cells with NM23-H1 overexpression, wild-type-H1 should inhibit the metastatic characterizations of the malignant cell while mutant H1 is likely to lose the suppressing effect. The defect of the anti-metastatic function would be correlated to the inactivated enzymatic activity of mutant H1. The $K_{12}Q$ mutant, harboring lesions in all three enzymatic activities, makes it difficult to determine the relevant biochemical mechanisms. However, the identification of the E_5A mutant in this study is promising, because it is the only mutant selectively deficient in exonulease activity. Thus, the E_5A mutant would provide the possibility to discover the relationship between the 3'-5' exonuclease activity and the metastasis-suppressing function of NM23-H1.

CHAPTER THREE

3'-5' EXONUCLEASE ACTIVITY OF NM23-H1 PLAYS A CRITICAL ROLE

IN SUPPRESSING *IN VIVO* SPONTANEOUS METASTASIS

3.1. Introduction

NM23-H1 proteins have been shown to possess multiple enzymatic activities, in which nucleoside diphosphate kinase (NDPK), histidine protein kinase (hisK) and 3'-5' exonuclease (3'-5' EXO) activities have been extensively investigated. Of these enzymatic activities, 3'-5' exonuclease activity of NM23-H1 was identified by our laboratory recently (Ma et al., 2004; Ma et al., 2002). However, the relevant biochemical mechanisms underlying metastasis suppressor function of NM23-H1 are not very clear yet. The 3'-5' exonuclease activity is a plausible candidate due to the association of the enzyme with DNA repair processes and the mutator phenotype often arises as a consequence of its deficiency (Shevelev and Hubscher, 2002). Moreover, accumulation of mutations is suggested to be required for metastatic progression which permits tumor cells to overcome barriers to achieve metastases (Loeb, 1991, 2001). Thus we hypothesize that 3'-5' exonuclease activity of NM23-H1 plays an important role in maintaining genomic stability and in turn suppressing metastatic progression of tumor cells. To test this hypothesis, we have generated a panel of NM23-H1 mutants, including $H_{118}F$ (NDPK⁻, hisK⁻, EXO⁺), $P_{96}S$ (NDPK⁺, hisK⁻, EXO⁺), $K_{12}Q$ (NDPK⁻, hisK⁻, EXO⁻) and E_5A (NDPK⁺, hisK⁺, EXO⁻). The metastasis-suppressing activities of these variant NM23-H1 mutants will be analyzed by *in vitro* and *in vivo* metastasis assays. Loss of anti-metastatic function will be related to the inactivated biochemical activity of NM23-H1 mutants. The 3'-5' exonuclease activity was selectively disrupted in the E_5A mutant, providing an insight into the role of this enzymatic activity in metastasis suppression. Furthermore, this panel of NM23-H1 mutants also includes the NDPK and histidine kinase deficient mutants ($H_{118}F$ and $P_{96}S$ respectively), the contribution of NDPK and histidine kinase activities to the metastasis suppressor function can be analyzed by the metastasis assays as well.

Metastasis can be quantified by *in vivo* assays. There are two types of xenograft metastasis assays, spontaneous and experimental (Welch, 1997). In a spontaneous metastasis assay, tumor cells are injected into tissue sites (i.e. subcutaneously, intradermally, intramuscularly, or into specific organs or tissues) which results in formation of a local tumor that will eventually give rise to spontaneous metastases. This assay measures the complete metastatic process but requires long post-injection time for completion. In an experimental metastasis assay, tumor cells are injected into the bloodstream of rodents and metastases form quickly and in greater numbers, but this assay circumvents the early steps of metastasis, such as local tumor growth and intravasation. Full characterization of any metastasis model system should include both assays. In our experimental design, a highly metastatic melanoma cell line 1205Lu was selected to measure the anti-metastatic characteristics of NM23-H1 by both *in vivo* metastasis assays. The melanoma cell line 1205Lu was established from lung metastatic lesions in mice after subcutaneous injection of WM793 cells, while the WM793 cell line from the vertical growth phase of melanoma represents premetastatic cells. The stably transfected 1205Lu cells with wild-type and mutant NM23-H1 variants were subcutaneously injected in spontaneous assay and intravenously injected in experimental assay. In both models, mice developed lung nodules, therefore recapitulating all the steps from primary solid tumor formation to metastatic spread.

3.2. Materials and Methods

3.2.1. Plasmids construction

cDNAs encoding the NM23-H1 mutants $K_{12}Q$, $P_{96}S$ and $H_{118}F$ were generated by the overlap extension modification of the polymerase chain reaction (PCR), as described (Ho et al., 1989). They were inserted in frame between the XhoI and EcoRI sites of the pCI-neo mammalian expression vector (Promega). The E_5A mutant was constructed using the QuikChange site-directed mutagenesis kit (Stratagene). The pCI vector carries the

cytomegalovirus (CMV) promoter for high level of DNA expression and the neomycin phosphotransferase gene for the selection of stable transfected clones. Additionally, in this vector the GFP is co-expressed with NM23-H1 in an IRES (Internal Ribosome Entry Segment) expression cassette. The cloned PCR products were sequenced by ACGT and Elim Biopharmaceutical Inc. to ensure that only desired mutations were present.

3.2.2. Animals

Female athymic nude mice (Harlan, *nu/nu;* 6-8 weeks old) were obtained. Care of mice, surgery and injection protocols were approved by the IACUC at the University of Kentucky Medical Center (protocol # 00319M2001 and 00801M2004). The mice were determined to be free from pathogens and caged in groups of four in facilities meeting National Institutes of Health guidelines. The mice were euthanatized by intraperitoneal injection of sodium pentobarbital (Nembutal, Sigma) at dose of 60 mg/kg.

3.2.3. Cell culture, stable transfection and flow cytometry

1205Lu melanoma cells were cultured in MCDB153/L15 medium (Sigma; v/v: 4/1) supplemented with $CaCl_2$ (2 mM), insulin (5 mg/ml) and 2% fetal bovine serum (FBS) (Gibco). 1205Lu melanoma cells were stable transfected with plasmid DNA of wild-type and mutant *nm23-H1* (Fugene 6, Roche) and selected by geneticin (G418, Life technologies; 250 µg/ml). Cells were sorted by fluorescence-activated cell sorting (FACS) using a FACS Calibur Flow Cytometer. The sorting procedure yielded more than 95% GFP fluorescent cells.

3.2.4. Spontaneous lung metastasis assay

The parent or variant H1-expressing 1205Lu cells were harvested by a brief exposure to PBS. Cell numbers and viability were examined using trypan blue. Single-cell suspensions of >90% viability were resuspended at 1 x 10^6 cells in 100 µl of Hank's balanced salt solution (Gibco). 2 x 10^6 1205Lu cells of each group were injected subcutaneously into the flank of athymic nude

mice. The growth of the tumors was monitored and measured at 3-day intervals using vernier caliper. Tumor volumes were calculated by the following formula: volume=0.52 x A x B^2, where A is the larger and B is the smaller axis (Tomayko and Reynolds, 1989). Mice were anesthetized under isoflurane and the primary tumors were removed when the tumor size reached 0.8-1 cm^3. The removed primary tumors were checked for fluorescence using Kodak Image Station 4000. The mice were raised for another 3 months to permit metastatic growth. At the end of the experimental period, mice were euthanatized and lung metastases were scored by counting metastatic nodules. The whole procedure of spontaneous metastasis assay is illustrated in Figure 9A.

3.2.5. Experimental lung metastasis assay

The metastatic potency of 1205Lu parent cells and variant NM23-H1 transfectants were also determined using an "experimental metastasis assay" (Kath et al., 1991). 2 x 10^6 parent cells or variant mutant H1-expressing 1205Lu cells (in a volume of 0.1 ml Hank's buffer) were injected into the lateral tail veins of nude mice. Animals were sacrificed after 1 month and the lungs were fixed in Bouin's solution and scored for metastatic nodules. As shown in Figure 9B, the procedure of experimental metastasis assay is exhibited.

3.2.6. Statistical analysis

The proportion of metastasis was compared among the seven groups by constructing a chi-square statistic for a 7 by 2 contingency table. If significant, group response rates will then be compared one to the other by chi-square statistics or Fisher's exact test for a series of 2x2 contingency tables. Statistical significance was determined if $P < 0.05$.

Figure 9. Illustration of procedures of *in vivo* metastasis assays.

(A) In spontaneous metastasis assay, 2×10^6 1205Lu parent or *nm23-H1* variant transfected cells were injected subcutaneously into the flank of nude mice. When the tumor size reached 0.8-1 cm^3, the primary tumors were removed and mice were continually raised for three months to permit formation of lung metastases. At the end of the experiment, mice were sacrificed and lung nodules were counted. (B) In experimental metastasis assay, 2×10^6 1205Lu parent or transfected cells were injected directly into tail vein of nude mice. One month later, mice were sacrificed and metastatic lung nodules were scored.

A.
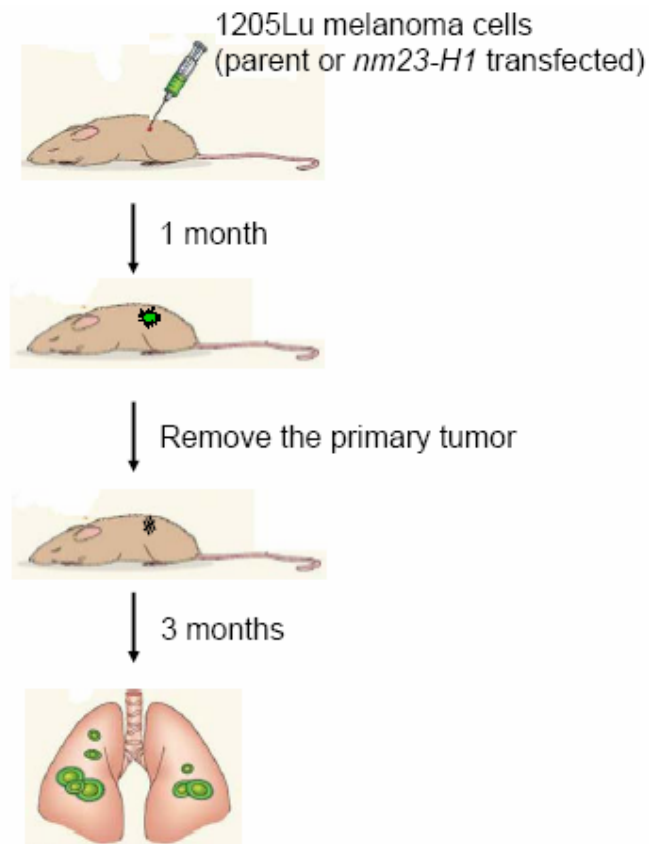
B.

1205Lu melanoma cells
(parent or *nm23-H1* transfected)

1 month

3.3. Results

3.3.1. NM23-H1 expression does not affect primary tumor growth of 1205Lu melanoma cells.

Parent and stably transfected 1205Lu cells with NM23-H1 variants were injected subcutaneously into athymic nude mice and the growth of primary tumors were monitored over time. The sizes of primary tumors were measured by calipers and after four weeks, tumor volumes reached 0.8-1.0 cm^3. As shown in Figure 10, the primary tumor formed by wild-type NM23-H1 transfected 1205Lu cells was not significantly different from that of parent cells, suggesting expression of wild-type-H1 had no inhibitory effect on primary tumor growth of 1205Lu cells *in vivo*. Once the size of primary tumor reached 0.8-1.0 cm^3, tumors were removed and mice were continually raised for another 3 months to form lung metastases.

Figure 10. NM23-H1 expression does not affect primary tumor growth.
2×10^6 parent and variant NM23-H1-expressing 1205Lu cells were subcutaneously injected on the flanks of mice to form primary tumors. The size of primary tumors was measured by calipers every 3-4 days. Primary tumor growth from wild-type NM23-H1, $H_{118}F$-H1 and $P_{96}S$-H1 transfected cells had no significant difference compared to that of 1205Lu parent cells. The tumor formed in $K_{12}Q$-H1- and E_5A-H1-transfected cells exhibited slower growth than parent cells after day 20, however, they still reached the target size of 0.8-1.0 cm^3 on day 30 (5 days later than other groups).
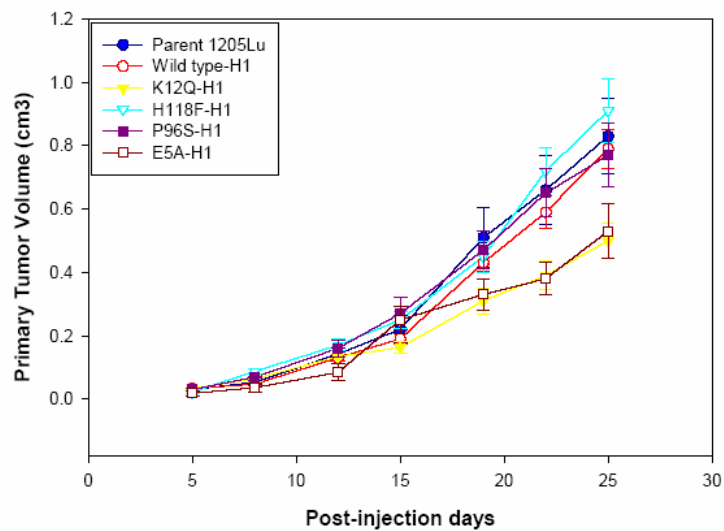
3.3.2. The E_5A and $K_{12}Q$ mutations disrupt metastasis suppressor activity of NM23-H1.

Three months after the primary tumors being removed, all mice were sacrificed and lungs were examined for metastatic nodules. Lung metastases were scored as plus or minus and metastasis rate was calculated by number of mice with lung metastasis over total number of mice in this group. As shown in Table 5, a 64% metastasis rate was observed in the parent 1205Lu cells, a relatively high penetrance for this cell line. Expression of the wild-type NM23-H1 significantly suppressed the spontaneous metastasis rate to 24%, consistent with its previously described metastasis suppressor activity (Table 5). Unexpectedly, the $P_{96}S$ mutant exhibited full metastasis suppressor activity (Table 5), in contrast with previous reports (Hartsough et al., 2002). However, the E_5A and $K_{12}Q$ mutations resulted in a nearly complete loss of suppressor activity (Table 5). The $H_{118}F$ mutant also exhibited less metastasis-suppressing activity than the wild-type, but the reduction failed to achieve statistical significance. As shown in Figure 11, the spontaneous lung metastases from 1205Lu parent cells and E_5A-H1 group were much more severe than that of the wild-type group.

Table 5. The $K_{12}Q$ and E_5A mutations result in complete loss of metastasis suppressor activity for NM23-H1. After primary tumors were excised, mice were raised for another 3 months to permit lung metastases. At the end of the experiment, all mice were sacrificed at the same day and lungs were examined for metastatic nodules. Metastasis rate in each group is presented as a percent of number of mice with lung metastasis/total mice number in this group.

1205Lu cell lines	# of mice with lung metastasis/ # of total mice[1]	Percentage rate
Parent	14/22	64[a,b]
WT-H1	9/37	24[c]
E_5A	13/26	50[a,b]
$K_{12}Q$	14/24	58[a,b]
$P_{96}S$	6/24	25[c]
$H_{118}F$	8/20	40[a,b,c]

[1]Qingbei Zhang and Marian Novak contributed to the data shown above.

[a,b,c] Values not sharing a common superscript are significantly different ($p < 0.05$).

Figure 11. Representative pictures of spontaneous lung metastases from 1205Lu parent cell group (a and b), wild-type-H1 group (c and d) and E$_5$A-H1 group (e and f).
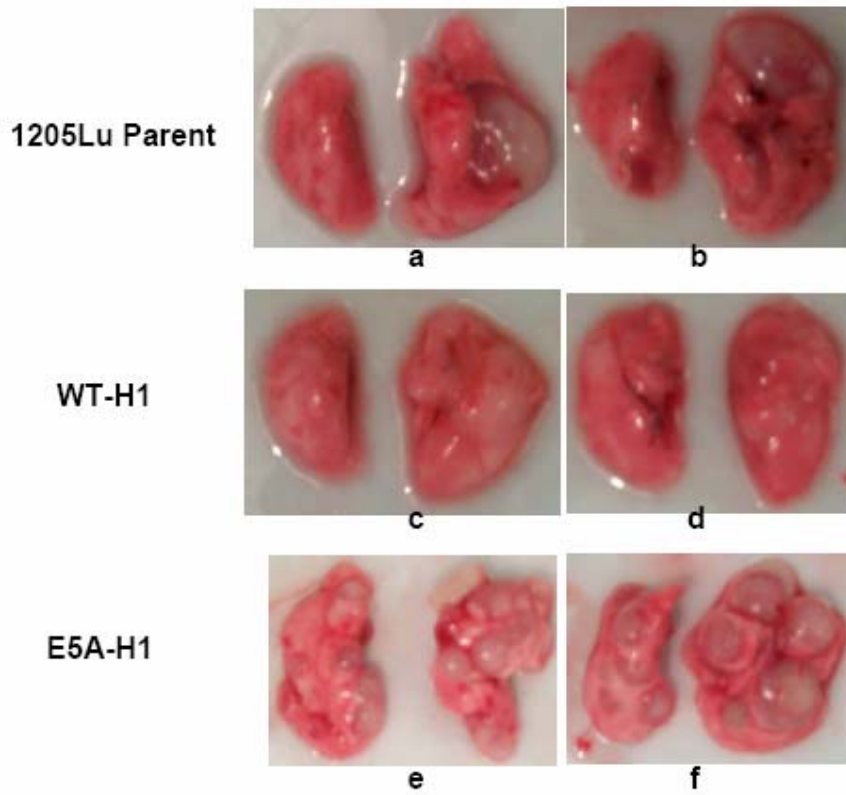
3.4. Discussion

The molecular mechanism(s) underlying the metastasis suppressor activity of NM23 proteins still remain controversial. Currently, the most widely accepted model involves the histidine kinase (hisK) activity of NM23-H1 as some evidence suggests that this enzymatic activity is necessary for inhibition of cell motility and suppression of Map kinase activation via phosphorylation of the kinase suppressor of Ras (KSR) in MDA-MB-435 breast carcinoma cells (MacDonald et al., 1996). However, direct evidence for the relevance of hisK to *in vivo* metastasis suppression has not been determined. In this study, we propose that the 3'-5' exonuclease activity of NM23-H1 plays an important role in suppressing metastasis by maintaining genomic integrity. However, an efficacious metastasis suppressor might be expected to exert multiple activities at multiple levels. Therefore, our hypothesis does not exclude the possibilities that other known enzymatic activities of NM23-H1 could also contribute to the anti-metastatic function. To this end, a panel of variant NM23-H1 mutants has been developed and used to systematically determine the relevant contributions made by each of the primary enzymatic activities of NM23-H1.

To assess the anti-metastatic function of NM23-H1, the human metastatic melanoma cell line 1205Lu was chosen as an experimental model in this project for a number of reasons. First, melanoma represents the prototypical setting for the metastasis suppressor NM23-H1, since the metastasis suppressor activity of NM23 was originally identified in the murine melanoma cell line K-1735 (Steeg et al., 1988). Second, 1205Lu cells exhibited highly metastatic characteristics in a number of *in vitro* and *in vivo* models. Third, orthotopic tumor inoculation (subcutaneous injection) of melanoma cells is easy to be performed on animals. Finally, and most importantly, my colleague has demonstrated that 1205Lu cells expressed very low amounts of NM23-H1 and NM23-H2 (Qingbei Zhang, Ph.D. dissertation, 2006), consistent with a classical model of reduced NM23 expression in melanoma metastases. This low level of NM23 expression also provides a low background upon which the anti-metastatic activity of wild-type and mutant NM23-H1 can be determined.

NM23-H1-expressing plasmids and pSV2neo were co-transfected into 1205Lu cell line. Stably transfected cells were selected by neomycin analogue G418 and enriched by sorting of GFP-fluorescent cells. Same intensity of GFP fluorescence in variant H1-transfected cells indicated that equal amount of NM23-H1 was expressed. To measure the anti-metastatic ability of wild-type and mutant NM23-H1, parent and variant NM23-H1-expressing 1205Lu cells were injected into athymic nude mice by standard approaches of spontaneous and experimental metastasis assays.

In the spontaneous metastasis model, forced expression of wild-type NM23-H1 had no effect on primary tumor growth of 1205Lu cells, but in $K_{12}Q$-H1 and E_5A-H1 overexpressed cells the primary tumor growths were slower than that of parent cells. However, subsequent replication of these studies by my colleague (Marián Novak) has demonstrated that there is, in fact, no statistical difference in primary tumor growth rates. Therefore, NM23-H1 still fits the definition of metastasis suppressor, by which it does not affect primary tumor growth when inhibiting tumor metastasis.

At the end of this experiment, wild-type NM23-H1 and $P_{96}S$ mutant significantly suppressed the spontaneous lung-metastasis rate of 1205Lu cells to 24% and 25% respectively, while the $K_{12}Q$ and E_5A mutants lost the metastasis-suppressing effects exhibited by the wild-type-H1 (Table 5). Based on these observations, the actions of these mutants on lung metastases need to be discussed one by one. -1- Since E_5A-H1 is an exonuclease-deficient mutant with full NDPK and hisK activities, loss of metastasis suppressor activity of this mutant would directly suggest that the 3'-5' exonuclease activity of NM23-H1 is required to suppress lung metastasis from melanoma lesion. -2- The histidine kinase activity of NM23-H1 seems not to contribute to the metastasis suppressor function, since the hisK-deficient $P_{96}S$ mutant still maintains the full anti-metastatic capacity. -3- The $H_{118}F$ mutant is deficient in both NDPK and hisK activities. Since the apparent loss of anti-metastatic activity with the $H_{118}F$ mutant was not statistically significant, relevance of the NDP kinase to anti-metastasis function could not be demonstrated. -4- The $K_{12}Q$ mutant lacks all three of these enzymatic activities and also disrupts the metastasis-inhibiting capacity. As discussed above, if either NDPK or hisK activity is not involved in the mechanism of metastasis suppression, 3'-5'

exonuclease must be necessary to suppress metastasis in 1205Lu melanoma cells, consistent with the result of the E$_5$A group. Taken together, all these results strongly indicate that 3'-5' exonuclease activity of NM23-H1 plays important roles in suppressing spontaneous lung metastasis in 1205Lu melanoma cells. In contrast with a previous report that the histidine kinase activity might mediate the metastasis suppressor function of NM23-H1 (Hartsough et al., 2002), in this study, it does not seem to be involved in this function.

In the experimental metastasis assays (performed by my colleagues Qingbei Zhang and Marián Novak) , the tail vein injection of 2x10^6 1205Lu parent cells led to an 87% of metastasis. However, unlike what we expected, overexpression of wild-type NM23-H1 didn't significantly inhibit the lung metastasis. These observations suggested that NM23-H1 lost the metastasis suppressor function when a large number of melanoma cells directly entered the blood system. These cells flowed to the lungs and were trapped within pulmonary capillaries, followed by intravascular proliferation and eventual colonization in the lung. In this process, early steps of the metastatic progression were omitted, including the loss of cellular adhesion, increased motility and invasion, entry and survival in the circulation. Therefore, the experimental metastasis accelerated the metastatic period and increased the metastatic efficiency. The observations that NM23-H1 was able to inhibit the metastasis in the spontaneous metastasis model but not in the experimental metastasis model suggested that NM23-H1 may mediate the suppressing effects on the earlier steps of metastasis. This idea is supported by our *in vitro* studies of 1205Lu cells, which showing that overexpression of wild-type NM23-H1 inhibited motility and invasion of the cells (Qingbei Zhang, Ph.D. dissertation, 2006). Another evidence is that forced expression of NM23-H1 inhibited anchorage independent growth in soft agar in MDA-MB-435 and MDA-MB-231 cells (McDermott et al., 2007). Furthermore, overexpression of NM23-H1 in human breast carcinoma cells led to the formation of basement membrane and growth arrest (Howlett et al., 1994), which also supported the idea that NM23-H1 performs a suppressor function in the early stages of metastasis.

Interestingly, the effects of NM23-H1 mutants on the *in vivo* spontaneous metastasis assay of 1205Lu cells were consistent with an *in vitro* assay developed in the Kaetzel laboratory using the non-metastatic melanoma cell line WM793 (performed by Qingbei Zhang and Marián Novak). The WM793 cell line was derived from a vertical growth phase (VGP) melanoma, a highly invasive but non-metastatic form of the disease. Expression of NM23 was undetectable in this cell line. This non-metastatic cell line can progress to a metastatic phenotype under strong selective pressure, such as culturing in protein-free (growth factor-free) medium (Kath et al., 1991). The unpublished data achieved by my colleagues demonstrated that forced expression of wild-type NM23-H1 significantly blocked the progression process of WM793 cells in protein-free medium. Moreover, similar to the pattern observed in 1205Lu cells, $K_{12}Q$ but not $P_{96}S$ mutant lost the effects of anti-progression exhibited by wild-type-H1. This observation further demonstrated that 3'-5' exonuclease activity of NM23-H1 is likely to mediate the biochemical mechanisms in metastasis suppression.

Evidence from *in vivo* spontaneous metastasis assay of 1205Lu cells and *in vitro* progression assay of WM793 cells strongly indicates that the 3'-5' exonuclease activity of NM23-H1 is important to suppress metastasis and metastatic progression of melanoma cells. The underlying mechanisms could be that 3'-5' exonuclease activity participates in DNA repair or other aspects of cellular function to maintain genomic integrity. The properties of NM23-H1 in maintenance of genomic stability will be addressed in next chapter.

CHAPTER FOUR
ANALYSIS OF DNA REPAIR ACTIVITY FOR *YNK1*, THE YEAST *SACCHAROMYCES CEREVISIAE* HOMOLOGUE OF METASTASIS SUPPRESSOR NM23

4.1. Introduction

Nucleoside diphosphate kinase (NDPK) catalyzes the transfer of a γ-phosphate between nucleoside triphosphate and nucleoside diphosphate via a "ping-pong" mechanism (Agarwal et al., 1978). NM23 is a highly conserved enzyme from prokaryotes to eukaryotes, with their three-dimensional structures showing remarkable similarity (Dumas et al., 1992), indicating that NDP kinase evolution is highly conservative. In addition to NDPK activity, NDP kinase has been determined to have a number of other important cellular and biochemical functions in different species.

NM23-H1 was first identified by virtue of its reduced expression in highly metastatic melanoma and breast carcinoma cells, and the ability of forced NM23-H1 expression to inhibit metastatic potential without significant impact on the transformed phenotype (Steeg et al., 1988). In addition to NDPK activity, NM23-H1 also exhibits both protein histidine kinase (HisK) (Freije et al., 1997) and 3'-5'exonuclease (3'-5'EXO) activities (Ma et al., 2004). Generally, enzymes that contain 3'-5' exonuclease activity are involved directly in DNA repair processes and maintenance of genomic stability (Shevelev and Hubscher, 2002). Here, we hypothesize that the loss of the 3'-5' exonuclease activity of NM23-H1 during tumor progression impairs genomic integrity, thereby enhancing metastatic potential.

Previous studies provide compelling evidence on the potential DNA repair functions of NM23. *Ndk*-disrupted strain of *Escherichia coli* exhibited a mutator phenotype with significantly increased frequencies of spontaneous mutations resistant to rifampicin and nalidixic acid (Lu et al., 1995). This is a direct evidence for the anti-mutator function of the prokaryotic homologue of NM23. In yeast mutagenesis studies, expression of *YNK1*, the budding yeast

homologue of NM23, was significantly increased in response to treatment with the DNA methylating agent methyl methanesulfonate (MMS) (Gasch et al., 2001). In addition, our unpublished data show that NM23-H1 accumulates and co-localizes with nuclear foci following the treatment with DNA damaging agents etoposide, cisplatin and UV radiation. UV radiation seems to have a stronger effect on this observation than etoposide and cisplatin. These DNA damage responses further suggest a DNA repair function of NM23-H1.

In an effort to quantify the contribution of NM23-H1 to DNA repair, we have initiated experiments in the yeast *Saccharomyces cerevisiae*. *S. cerevisiae* provides an excellent eukaryotic model for DNA repair research, since knockout strains are available for essentially all genes including those involved in DNA repair mechanisms. These characteristics of *S. cerevisiae* provide a genetic model for rapid and convenient analysis of the role of *YNK1* in DNA repair. In this project, we measured the impact of deletion of the *YNK1* on the mutation rate in *S. cerevisiae*.

4.2. Materials and Methods

4.2.1. Yeast strains and media

The single mutant strains (Open Biosystems) used as parent strains in this study were derived from BY4741 or BY4742 wild-type strain and their genotypes are listed in Table 6. The ORF for each gene of interest was replaced with a KanMX-selectable marker by a PCR-based strategy. The double mutant strain was constructed by crossing *ynk1:: kanMX* mutant with an isogenic strain harboring another deletion in one of *DDC1*, *RAD17*, *MEC3*, *MSH2*, and *RAD27* genes. Genotypes were verified for resultant haploid derivatives of each mutant strain by PCR analysis using primer pairs specific for either the wild-type or mutant allele. Yeast strains were grown in standard media including yeast extract/peptone/dextrose (YPD) medium or synthetic drop-out medium (SD) lacking the appropriate amino acid. Canavanine-resistant mutants (Can^r) were selected on SD arginine-dropout plates containing 60 mg/liter L-canavanine sulfate (Sigma).

Table 6. *S. cerevisiae* strains used in this study

Strain	Genotype
BY4741	a. *his3Δ1 leu2Δ0 met15Δ0 ura3Δ0*
BY4742	α. *his3Δ1 leu2Δ0 lys2Δ0 ura3Δ0*
ynk1	a. *his3Δ1 leu2Δ0 met15Δ0 ura3Δ0 ynk1::kanMX*
ddc1	α. *his3Δ1 leu2Δ0 lys2Δ0 ura3Δ0 ddc1::kanMX*
rad17	α. *his3Δ1 leu2Δ0 lys2Δ0 ura3Δ0 rad17::kanMX*
mec3	α. *his3Δ1 leu2Δ0 lys2Δ0 ura3Δ0 mec3::kanMX*
msh2	α. *his3Δ1 leu2Δ0 lys2Δ0 ura3Δ0 msh2::kanMX*
rad27	α. *his3Δ1 leu2Δ0 lys2Δ0 ura3Δ0 rad27::kanMX*
ynk1 ddc1	*his3Δ1 leu2Δ0 met15Δ0 ura3Δ0 ynk1::kanMX ddc1::kanMX*
ynk1 rad17	*his3Δ1 leu2Δ0 lys2Δ0 ura3Δ0 ynk1::kanMX rad17::kanMX*
ynk1 mec3	*his3Δ1 leu2Δ0 ura3Δ0 ynk1::kanMX mec3::kanMX*
ynk1 rad27	*his3Δ1 leu2Δ0 lys2Δ0 ura3Δ0 ynk1::kanMX rad27::kanMX*
ynk1 msh2	*his3Δ1 leu2Δ0 met15Δ0 ura3Δ0 ynk1::kanMX msh2::kanMX*

4.2.2. UV sensitivity assay

Individual colonies were inoculated into 1 ml of YPD medium and grown overnight with shaking at 250 rpm at 30°C to a density of 2 x 10^8 cells/ml. 100 μl of the appropriate cell dilution were plated in triplicate on YPD agar plates to assess cell survival. Within an hour of plating, cells were exposed to UV light on a time course. After UV exposure the plates were immediately stored in incubator at 30°C. Cell viability was the fraction of plated cells which gave visible colonies after 3 to 4 days of growth on YPD plates. Each data point corresponds to the mean of 3 independent experiments, and error bars represent the standard deviation in Figure 14.

4.2.3. CAN1 forward mutation assay

Individual colonies were inoculated into 1 ml of YPD medium and grown overnight with shaking at 250 rpm at 30°C to a density of 2 x 10^8 cells/ml. Cells were washed once with sterile distilled water and then resuspended in 1 ml of sterile 50 mM potassium monohydrogen/dihydrogen phosphate buffer, pH 7.0. For determination of Can^r mutation rates, 100 μl of an appropriate dilution (~100 cells) was plated on SD-arginine (SD-arg) medium and 200 μl of the remaining culture (~4 x 10^7 cells) was plated on SD-arginine containing canavanine (SD+can) medium. Plates were incubated for 5 days at 30°C, and the number of Can^r colonies was counted. Mutation rates were determined by the method of the median (Lea and Coulson, 1948), and 95% confidence intervals (CIs) were calculated as described in this reference. At least 10 independent cultures were used for all measurements of mutation rate.

4.2.4. MMS-induced mutagenesis

1 ml of cells was grown overnight in YPD medium, harvested and resuspended in 1 ml of 50 mM potassium phosphate, pH 7.0. Methyl methanesulfonate (MMS) was added to 0.1% and cells were incubated at 30°C with shaking for 40 min. An equal volume of 10% ice cold sodium thiosulfate was added to the culture and incubated for 10 min. The cells were

harvested, washed twice with sterile water and then suspended in 50 mM potassium phosphate, pH 7.0. Cells were diluted and plated on SD plates followed by the standard *CAN1* mutation assay.

4.2.5. UV-induced mutagenesis

1 ml of cells was grown overnight in YPD medium, harvested and resuspended in 1 ml of 50 mM potassium phosphate, pH 7.0. Cells were diluted and plated on SD-arg and SD+can medium. The SD+can plates were then exposed to UV light at a dose of 70% cell viability. All plates were incubated for 5 days at 30°C, and the rest procedure followed the standard *CAN1* mutation assay.

4.2.6. Fluctuation analysis

To determine CAN1 mutation frequency, at least 10 independent cultures were analyzed in each experiment and each experiment was repeated for at least two times. The method of the median (Lea and Coulson, 1948) was used to calculate CAN1 mutation rate and 95% confidence interval of each rate.

4.2.7. Sequence analysis of CAN1 mutation spectra

Independent Can^r colonies were isolated, and genomic DNA was extracted with yeast DNA extraction kit (Pierce). *CAN1* gene was amplified by PCR and sequenced at UK Advanced Genetic Technologies Center. Sequencing analysis was done using NCBI Blast request.

4.3. Results

4.3.1. *ynk1*Δ strain displays a UV-induced mutator phenotype.

*ynk1*Δ strain didn't display defects in growth rate, spore formation, mating ability or morphology (Fukuchi et al., 1993). In our studies, *ynk1*Δ mutants exhibited no increase in spontaneous mutation rate than wild-type strain from the described *CAN1* forward mutation assay. Then both wild-type and *ynk1*Δ strains were treated with DNA damaging agents MMS and UV radiation. 0.1% MMS induced an 11-fold increase in mutation rate at *CAN1* locus in *ynk1*Δ strain, compared to an 8-fold mutation increase in wild-type strain (Figure 12A). However, the ratio of UV-induced mutation rate to spontaneous mutation rate at *CAN1* locus in *ynk1*Δ strain was 13:1, while wild-type strain exhibited a 5-fold increase in UV-induced mutation rate. The fold increase rate (13:5) between *ynk1*Δ and wild-type strains was significantly different analyzed by one way ANOVA (Figure 12B). In addition, the UV-induced mutator phenotype was reproducible in *ynk1*Δ spore cells generated from double mutants, in which the fold increase (UV-induced mutation rate/spontaneous mutation rate) was consistently 2-3 fold higher than their wild-type sporemates (data not shown). These results suggested that *YNK1* deletion led to a moderate, but significant repair deficiency to UV-induced DNA damage.

Figure 12. Deletion of *YNK1* results in increased mutations in response to MMS and UV insults. The *CAN1* forward mutation rate was measured in both wild-type and *ynk1Δ* strains under either spontaneous conditions or following the treatment with DNA damaging agents MMS or UV. (A) 0.1% MMS was used to induce *CAN1* mutation rate. (B) A dose of 192 J/m^2 of UV radiation was used to induce *CAN1* mutation rate. Both treatments resulted in a 70% viability rate for both strains. 10 independent cultures were used for all measurements and at least three experiments were performed, data was analyzed by one way ANOVA.

A.
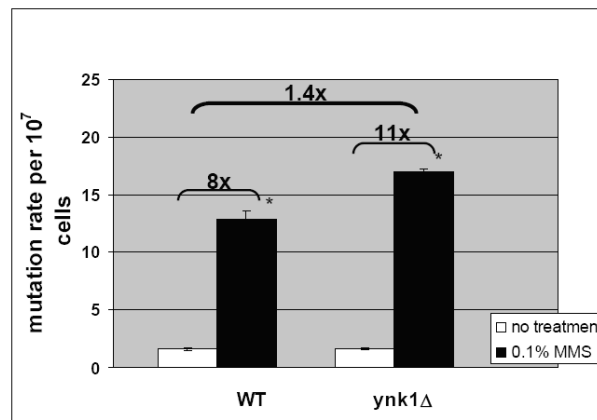
B.
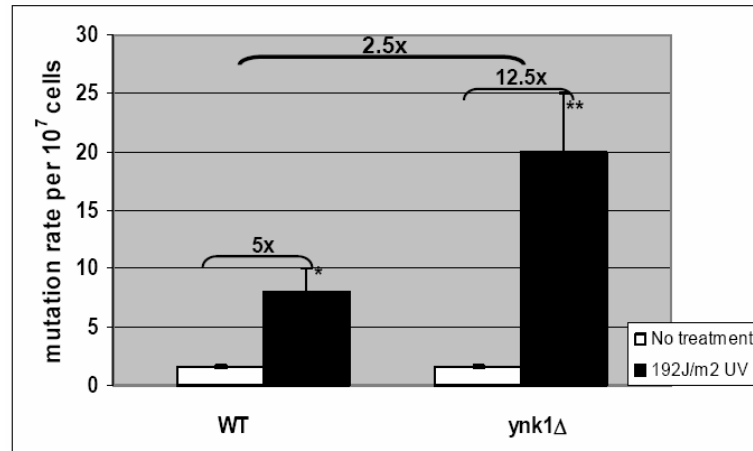
4.3.2. *CAN1* mutation spectra analysis

CAN1 encodes an arginine permease (Ahmad and Bussey, 1986), and any loss-of-function mutation at this locus confers resistance to canavanine. To better understand the accumulation of mutations in the *ynk1*Δ strain, the mutation spectra for both of wild-type and *ynk1*Δ strains was determined by sequencing the *CAN1* gene from approximately 20 independent Can[r] isolates. As shown in Table 7, under basal conditions, the Can[r] mutations in wild-type cells were base substitutions (59%) and deletions (23%), while *ynk1*Δ cells had 70% of base substitutions and 6% of deletions. In UV-irradiated wild-type cells the frequency of base substitutions was 53% and deletion 21%, which resembled that of no treatment. The UV-irradiated *ynk1*Δ cells demonstrated 70% of base substitutions and 15% of frameshifts. Notably, the frameshift events were only shown in this group. In addition, it's interesting to note that a frequency of thymidine (T) tract (at least three T in order) mutation alterations in this group was as high as 65%, which was remarkably higher than any other groups (e.g., 18% in wild-type cells with no treatment, 24% in *ynk1*Δ cells with no treatment and 26% in UV-irradiated wild-type cells).

Table 7. CAN1 forward mutation spectrum

Genotype	Event	Can^r	
		Mutation	Frequency
Wild type	Base substitution	G→T	2/17
		G→A	4/17
		T→G	1/17
		C→A	1/17
		C→T	1/17
		T→C	1/17
		Total	10/17(59%)
	Frameshift		0/17(0%)
	Deletion	29 bp	2/17
		~100 bp	1/17
		~200 bp	1/17
		Total	4/17(23%)
	Complex	ACACCACAG→CACAA	1/17(6%)
	No mutation		2/17(12%)
ynk1∆	Base substitution	G→A	3/17
		T→A	1/17
		A→T	1/17
		C→A	2/17
		C→T	3/17
		C→G	2/17
		Total	12/17(70%)
	Frameshift		0/17(0%)
	Deletion	~200 bp	1/17(6%)
	Complex		0/17(0%)
	No mutation		4/17(24%)
Wild type with UV treatment	Base substitution	G→A	2/19
		G→T	3/19
		T→C	3/19
		C→A	1/19
		C→G	1/19
		Total	10/19(53%)
	Frameshift		0/19(0%)
	Deletion	CGAA→C∆AA	1/19
		TTTAT→TTT∆T	1/19
		~150 bp	1/19
		~350 bp	1/19
		Total	4/19(21%)
	Complex	AAATTA→TAATTT	1/19
		CATTGCGCTC→TATGCGCTT	1/19
		Total	2/19(10%)
	No mutation		3/19(16%)

ynk1Δ with UV treatment	Base substitution	G→A	4/20
		G→T	2/20
		T→A	3/20
		C→T	3/20
		A→G	1/20
		C→A	1/20
		Total	14/20(70%)
	Frameshift	T4→T2	1/20
		T5→T6	1/20
		T6→T7	1/20
		Total	3/20(15%)
	Deletion	TTTTCTT→ TTTTΔTT	1/20(5%)
	Complex	(TATTT)2→(T)11	1/20(5%)
	No mutation		1/20(5%)

4.3.3. The double deletion between *YNK1* and 9-1-1 component causes a decrease in UV-induced mutagenesis.

Since redundancy of DNA repair mechanisms exist in cells, loss of one gene function can be compensated by a separate pathway. At this point, to study the possible interactions of *YNK1* with other DNA repair mediators, double knockout mutants were generated in *ynk1*Δ background, which harbored a second deletion in a variety of known DNA checkpoints or DNA repair genes (*DDC1*, *RAD17*, *MEC3*, *RAD27 and MSH2*). Ddc1p, Rad17p, and Mec3p proteins form a heterotrimeric ring, with similar structure to proliferating cell nuclear antigen (PCNA) in *S. cerevisiae* (Majka and Burgers, 2003; Thelen et al., 1999). Their human homologues are RAD9, RAD1, and HUS1 respectively (9-1-1 complex). The 9-1-1 complex is a DNA damage checkpoint and causes cell cycle arrest in response to DNA damage (Kondo et al., 1999). Our microarray analysis has identified an elevated HUS1 expression in association with the loss of NM23 in metastatic cell lines.

The double mutant strain was generated by crossing a *ynk1*Δ mutant with another knockout mutant (e.g. *rad17*Δ) and four isogenic spores (e.g. wild-type, *ynk1*Δ, *rad17*Δ and *ynk1*Δ *rad17*Δ) were isolated from a double knockout diploid cell. The mutator phenotypes of the generated mutant cells were analyzed by *CAN1* forward mutation assay and compared with their wild-type counterparts. Under spontaneous conditions, *CAN1* mutation rates of *rad17*Δ, *mec3*Δ and *ddc1*Δ mutants exhibited 2.5-fold, 2.3-fold and 2.4-fold respectively higher than the wild-type cell (Table 8), consistent with previous study (Paulovich et al., 1998). As expected, the *ynk1*Δ *rad17*Δ, *ynk1*Δ *mec3*Δ and *ynk1*Δ *ddc1*Δ double mutants displayed similar mutation rates as the *rad17*Δ, *mec3*Δ and *ddc1*Δ single mutants, since the deletion of *YNK1* didn't affect the spontaneous mutation rate compared to wild-type cell (Table 8). Meanwhile, the 9-1-1 single mutants and double mutants were treated with UV radiation at different low doses according to their 70% UV viable rate. Compare to UV-irradiated wild-type cells, UV-induced mutation rate of 9-1-1 single mutants was reduced by about 50%. The UV-induced mutation rate of *ynk1*Δ *ddc1*Δ, *ynk1*Δ *rad17*Δ and *ynk1*Δ *mec3*Δ double mutants was close to

the *ddc1Δ*, *rad17Δ* and *mec3Δ* single mutant, but 70-80% lower than the *ynk1Δ* cell (Table 8).

Table 8. Forward mutation rates at the *CAN1* locus in wild-type and mutant strains.

Strain	Can^r mutation rate per 10^7 cells (fold increase)	
	spontaneous	UV-induced
Wild type	1.6 (1)	8 (1)
ynk1Δ	1.6 (1)	20 (2.5)
ddc1Δ	3.9 (2.4)	3.2 (0.4)
ynk1Δ ddc1Δ	4.0 (2.5)	5.5 (0.7)
rad17Δ	4.0 (2.5)	4.4 (0.6)
ynk1Δ rad17Δ	4.0 (2.5)	3.5 (0.4)
mec3Δ	3.6 (2.3)	4.8 (0.6)
ynk1Δ mec3Δ	5.2 (3.3)	5.7 (0.7)
rad27Δ	89 (56)	46 (5.8)
ynk1Δ rad27Δ	60 (38)	32 (4)
msh2Δ	28 (18)	24 (3)
ynk1Δ msh2Δ	34 (21)	34 (4.3)

Mutation rates shown here are the averages of at least two independent experimental sets. Fold increases in mutation rates compared to wild type are indicated in parentheses.

4.3.4. Deletion of *YNK1* does not affect UV sensitivity of the *ddc1Δ*, *rad17Δ* or *mec3Δ* mutant.

UV sensitivity of the *ynk1Δ ddc1Δ*, *ynk1Δ rad17Δ* and *ynk1Δ mec3Δ* double mutants was measured at gradient UV doses. As shown in Figure 13, *ynk1Δ* mutants did not exhibit more sensitivity than wild-type strain. The *ddc1Δ*, *rad17Δ* or *mec3Δ* single mutants were very sensitive to the killing effects of UV radiation, as previously reported (Longhese et al., 1997; Paulovich et al., 1998). However, the deletion of *YNK1* did not affect the UV sensitivity of *ddc1Δ*, *rad17Δ* and *mec3Δ* mutant in our studies.

Figure 13. Deletion of *YNK1* does not affect UV sensitivity of the wild-type cell and the 9-1-1 mutant. Cell viability was measured in wild-type, *ynk1Δ, ddc1Δ, rad17Δ, mec3Δ* and the corresponding double mutants, following UV exposure at a gradient dose.

A.
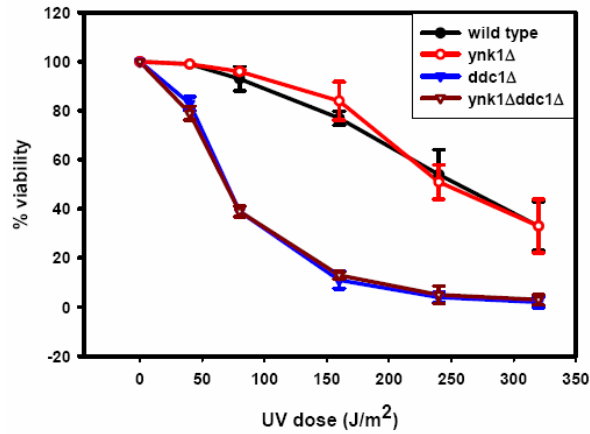
B.
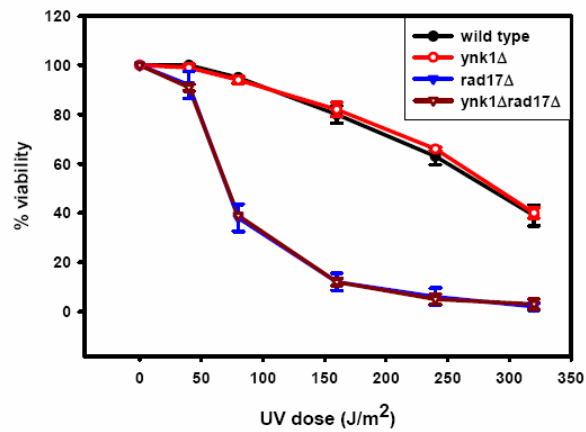
C.
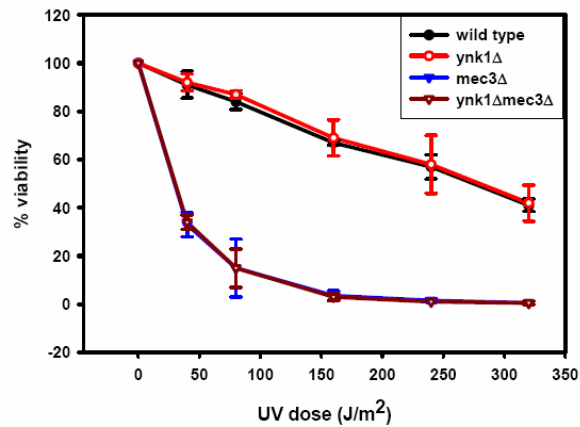
4.3.5. Characterization of the Can^r mutations of the *ynk1Δ rad27Δ* and *ynk1Δ msh2Δ* double mutants

S. cerevisiae RAD27 (homologue of human FEN1) proteins exhibited a 5'-3' exonuclease activity and an endonuclease activity involved in DNA replication and repair (Harrington and Lieber, 1994; Qiu et al., 2001). *rad27* mutants displayed a strong spontaneous mutator phenotype and showed increased rates of chromosome instability (Tishkoff et al., 1997). To examine the relationship between *YNK1* and *RAD27*, a *ynk1 rad27* double knockout mutant was constructed by crossing a *ynk1Δ* mutant to an isogenic *rad27Δ* mutant and dissecting tetrads from the resulting diploid. In comparison to the wild-type cell, deletion of *RAD27* caused a significantly greater increase in the spontaneous Can^r mutation rate (56-fold higher), which was consistent with previous studies (Tishkoff et al., 1997). The mutation rate in *ynk1Δ rad27Δ* mutant was 30% lower than *rad27Δ* mutant. With UV dose of 70% viable rate, the *rad27Δ* mutants had a 5.8-fold higher Can^r mutation rate than the wild-type strain, while the *ynk1Δ rad27Δ* double mutants displayed a Can^r mutation rate (3.2×10^{-6}) situated between *ynk1Δ* (2.0×10^{-6}) and *rad27Δ* (4.6×10^{-6}) single mutants (Table 8).

The products of mismatch repair genes *MSH2*, *MSH3* and *MSH6* in *S. cerevisiae* (MutS homologue of *E. coli*) form two complexes, Msh2p-Msh6p complex and Msh2p-Msh3p complex (Kolodner, 1996; Marsischky et al., 1996). They bind and function in the repair of base-base and insertion/deletion mispairs, and reduce the accumulation of mutations during DNA replication. To study the relationship between *YNK1* and *MSH2*, a *ynk1 msh2* double knockout mutant was constructed. Mutagenesis analysis showed that *msh2Δ* mutants exhibited increased Can^r mutations (18-fold higher) than wild-type cells, consistent with previous reports (Lau et al., 2002). The *ynk1Δ msh2Δ* double mutants showed a slight increase in spontaneous mutation rate compared to *msh2Δ* single mutants. Following the UV treatment, the *msh2Δ* mutants displayed a similar mutator phenotype as the *ynk1Δ* mutants (3-fold higher than wild-type), while the *ynk1Δ msh2Δ* double mutants showed a small additive effect. The effects of the deletion of *YNK1* and *MSH2* on UV-induced mutagenesis seemed to be added (Table 8).

73

4.4. Discussion

UV irradiation leads to DNA damage, primarily due to covalent linkage between adjacent pyrimidines. Such photoproducts block the progression of DNA polymerases and are potentially mutagenic. Nucleotide excision repair proteins are recruited to the site of the lesion and repair the damage in an error-free manner. This form of DNA repair reduces the mutation frequency induced by UV irradiation. If the damage persists when the DNA is replicated in S-phase of the cell cycle, translesion synthesis (TLS) is activated using an error-prone mechanism that involves the non-processive DNA polymerase zeta (Polζ) (McGregor, 1999). Polζ is consists of two subunits, catalytic subunit *REV3* and regulatory subunit *REV7* (Nelson et al., 1996). Polζ is required for the induction of mutations and Polζ mutants caused a decrease in UV-induced mutagenesis. Recent studies demonstrated that the *MEC3* and *DDC1* subunits of the 9-1-1 complex physically and functionally interacted with the *REV7* subunit of the Polζ, and the complex was required to stably recruit Polζ onto damaged DNA (Sabbioneda et al., 2005). This evidence provides an explanation for reduction in UV-induced mutagenesis in yeast 9-1-1 single mutants.

ynk1Δ strains displayed a significant UV-induced mutator phenotype that was assessed by measuring resistance to the toxic arginine analog canavanine, which suggests that *YNK1* is likely to play an important role in interacting with the UV damaged DNA. The Can[r] mutation spectrum indicates that the mutations in the *ynk1Δ* strain primarily resulted from nucleotide mis-incorporation and frameshift events, which can increase the frequency of DNA polymerase slippage, therefore enhancing the mutation rate. We suggest three possible explanations for the DNA damage-dependent anti-mutator function of *YNK1*: 1) *YNK1* possibly functions as a redundant 3'-5' exonuclease involved in DNA damage repair pathway; 2) *YNK1* is likely to be a redundant 3'-5' exonuclease facilitating DNA polymerase fidelity; 3) the NDPK activity of *YNK1* maintains the intracellular nucleotide balance, as the increased dCTP content has been suggested to result in the mutator phenotype in *ndk* deficient *E. coli* strain (Lu et al., 1995).

Nucleotide excision repair (NER) is primarily implicated in repair of UV-induced DNA damage by an error-free manner. *YNK*1 could possibly be

involved in the NER pathway by functioning as a redundant 3'-5' exonuclease to reduce mutations. The potential relationship of *YNK1* and DNA damage checkpoints (*DDC1*, *RAD17*, *MEC3*) or DNA repair enzymes (*RAD27 and MSH2*) was probed by mutation rate measurements in a double knockout strain. The effect of *YNK1* in UV-induced mutagenesis is suppressed in *ynk1∆ ddc1∆*, *ynk1∆ rad17∆* and *ynk1∆ mec3∆* double mutants, suggesting that *YNK1* is not likely to be involved in the 9-1-1 clamp regulated pathway. Rad27p, a structure-specific endo/exonuclease, plays an important role in DNA replication through Okazaki fragment maturation and DNA repair of 5'-blocked ends (Tishkoff et al., 1997). Based on the decrease in mutation rates of *ynk1∆ rad27∆* double mutants compared to *rad27∆* single mutants, *YNK1* does not seem to coordinately interact with *RAD27*. However, the majority of Can^r mutations in *ynk1∆* strain are consistent with the mutation spectrum in *msh2∆* mutants, changing from single nucleotide mis-incorporations and single/double-base frameshift events. Also, *ynk1∆ msh2∆* mutants display a small additive effect on the generation of mutations. This evidence suggests that *YNK1* is possibly involved in the mismatch repair pathway, exercising mispaired bases as a redundant 3'-5' exonuclease in response to DNA damage.

The *YNK1* amino acid sequence is highly homologous to NM23-H1, which suggests that NM23-H1 could also function as an anti-mutator and play an important role in mutations avoidance in humans, although direct evidence about the impact of NM23 expression on mutation rate in mammalian cells is lacking at present. Consistent with the putative DNA repair function of NM23-H1 is our observation of accumulation of NM23 within subnuclear foci following treatment with the DNA damaging agents etoposide, cisplatin and UV radiation. Collectively, these lines of evidence strongly support our hypothesis that NM23-H1 plays a critical role in maintaining genomic integrity in the tumor cells, reducing the accumulation of mutations during tumor metastasis pathway. Together, this study contributes to our understanding of the mechanisms underlying the metastasis suppressor activity of NM23-H1.

CHAPTER FIVE
GENERAL DISCUSSION

5.1. Conclusions and Discussion

Genetic instability results in a global increased mutation rate in a cell, which is termed "mutator phenotype". This idea was applied to carcinogenesis in 1976 by Nowell, who suggested that genetically unstable cells produce "successful" mutant clones for malignant process during tumor evolution (Nowell, 1976). In other words, the accumulated genetic changes during tumor progression might lead to an increasingly aggressive phenotype and metastasis ultimately. Since the fidelity of DNA synthesis and DNA repair play important roles in maintaining genomic integrity, loss of these functions increase genomic instability and enhance cancer risk (Sieber et al., 2003). 3'-5' exonucleases have an essential role in DNA replication and DNA repair by excising mismatched or modified nucleotides to maintain genomic integrity. At least 11 human proteins have been reported to exhibit 3'-5' exonuclease activity, which are either associated with polymerase (for instance, polymerases γ, δ and ε) or autonomous (such as, TREX1, TREX2, RAD1, RAD9, MRE11, APE1, p53 and VDJP) (Shevelev and Hubscher, 2002). Defects in the proofreading activity of the 3'-5' exonucleases could cause dramatic consequences in a cell. For instance, -1- a defective proofreading function of an autonomous 3'-5' exonuclease (dnaQ) in *E. coli* led to cell inviability due to excessive error rates (Fijalkowska and Schaaper, 1996). -2- A strong mutator phenotype in *S. cerevisiae* was induced owing to deficient proofreading in combination with defective mismatch repair (Morrison et al., 1993). -3- The loss of polymerase δ proofreading function can even lead to cancer in mice (Goldsby et al., 2001). Taken together, these data indicate that the 3'-5' exonucleases play important roles in decreasing the mutation frequency and possibly inhibiting the tumorgenicity and metastatic potential.

NM23-H1, the first metastasis suppressor, has been recently identified to possess 3'-5' exonuclease activity by our laboratory (Ma et al., 2004). NM23 proteins exhibit multiple enzymatic activities, consistent with its multiple functions in many aspects of cell signaling. Currently, at least three distinct

76

enzymatic activities of NM23-H1 are under active investigations for the relevant mechanism underlying metastasis-suppressing effects of NM23-H1. The 3'-5' exonuclease activity of NM23-H1 represents a very plausible candidate, as other well known 3'-5' exonucleases are indeed implicated in mechanisms of DNA repair. Moreover, the NDPK activity should also be considered, in light of its potential role in maintaining balance in nucleotide pool sizes. However, the histidine kinase activity of NM23-H1 might not be relevant, since this apparent protein kinase activity could be an artifact resulting from the presence of contaminating [γ-^{32}P]ATP. The details will be discussed later in this chapter.

Some evidence has been collected to suggest a role of NM23-H1 in DNA repair. First, our laboratory has observed that nuclear translocation and nuclear foci formation of NM23 proteins were responsive to DNA damaging agents cisplatin and etoposide (Kaetzel et al., 2006). This is a typical phenotype of DNA repair responses. Second, our laboratory has also observed that multiple DNA repair genes (Rad51, HUS1, MLH1, BRCA1, PCNA, FEN1, DNA polymerase θ and methyl-CpG binding protein) were coordinately downregulated in two metastatic cell lines with NM23-H1 overexpression (Kaetzel et al., 2006). This observation reflects that genomic instability is associated with the NM23-deficient state. Third, the mutator phenotype in NDPK-null *E. coli* (Lu et al., 1995) provided a direct evidence for a potential anti-mutator activity in a prokaryotic cell. Based on such evidence, some important questions arose to us: Does the 3'-5' exonuclease activity mediate the metastasis suppressor activity of NM23-H1? If so, what specific mechanism is involved? Is DNA repair activity involved in the anti-metastatic function of NM23-H1? And, what kind of DNA repair pathway is regulated?

To address these important issues, a panel of NM23-H1 mutants with selective enzymatic lesions have been constructed, characterized and expressed in human melanoma cell lines. The transfected melanoma cells have been conducted metastasis assays *in vitro* and *in vivo*. In addition, the role of *YNK1* (the yeast homologue of NM23) in DNA repair and maintenance of genomic integrity has been assessed by measuring the impact of ablation of the *YNK1* gene on mutation rates in *S. cerevisiae*. Hopefully these studies

will contribute to a further understanding of the anti-metastatic functions of NM23-H1.

5.1.1. Site-directed mutagenesis identifies Glu_5 and Lys_{12} are necessary for the 3'-5' exonuclease activity of the metastasis suppressor NM23-H1

To study the biochemical activity of NM23-H1 in metastasis suppression, our laboratory initiated the site-directed mutagenesis assay of NM23-H1. Previous results have shown that $K_{12}Q$-H1 mutant lost both NDP kinase and 3'-5' exonuclease activities, and $H_{118}F$-H1 mutant only inhibited NDP kinase activity (Ma et al., 2004). In this study, we demonstrated that both $K_{12}Q$ and $H_{118}F$ mutants also disrupted the histidine kinase activity. In addition, to completely develop a panel of NM23-H1 mutants for characterization of the 3'-5' exonuclease active site and identification of the relevant enzymatic activities to the metastasis suppressor funciton, more residue substitutions of NM23-H1 have been generated in this study. Previously, the $K_{12}Q$ mutant was the only variant deficient in 3'-5' exonuclease activity. In this study, we identified that the E_5A mutant also significantly disrupted the 3'-5' exonuclease activity of wild-type-H1 without markedly affecting other enzymatic activities. As the only variant selectively deficient in the exonuclease activity, E_5A has the potential to provide insights into this enzymatic activity in DNA repair. Although both Glu_5 and Lys_{12} are required for the 3'-5' exonuclease activity of NM23-H1, whether they might be coordinate for the enzymatic activity is not known yet. However, they are at opposite ends of β1 sheet, suggesting that the β1 sheet of NM23-H1 is important in binding and cleaving DNA substrate.

5.1.2. The histidine kinase activity of NM23-H1 might be artifactual

In the histidine protein kinase assay (performed by Robert McCorkle), NM23-H1 proteins were autophosphorylated at the residue His_{118} by incubation with $[\gamma\text{-}^{32}P]ATP$, and the unbound ATP was diluted and rinsed off by successive rounds of ultrafiltration. Then the phosphorylated NM23-H1 was subsequently incubated with NM23-H2, the target protein of this assay.

The phospho-NM23-H2 was visualized by gel electrophoresis and phosphorimaging. A coordinate reduction in both NDPK and hisK activities was shown among all of the mutants $K_{12}Q$, $Y_{52}A$, $P_{96}S$, and $H_{118}F$. This is difficult to explain, as the binding pockets for such disparate kinase substrates (nucleoside diphosphates versus proteins) should be quite different. An alternative explanation posed by Postel (Levit et al., 2002) is that the apparent protein kinase activity of NM23-H1 may be an artifact resulting from the presence of trace amounts of [γ-^{32}P]ATP in the reaction mixtures. This contaminating [γ-^{32}P]ATP could come from the produced ADP that is recycled by the nucleoside diphosphate kinase reaction. Thus, phosphorylation of the target protein (NM23-H2) is not a result of direct phosphotransfer from the phospho-NM23-H1 but rather a consequence of generation of [γ-^{32}P]ATP from the produced ADP. Since nanomolar concentrations of contaminating ADP can trigger the phosphotransfer cascade (Levit et al., 2002), the contaminating ATP is not easily detected. In this experiment, the unbound ATP represents less than 5% of that bound to NM23-H1. The contaminating ATP may function more as a catalyst in this phosphotransfer cascade than a donor supplying the phosphoryl groups. Since this histidine kinase assay was conducted in parallel with the metastasis assay, we did not realize this possibility at the time we performed the metastasis assay. However, this finding indicates that the previously proposed role of the histidine kinase activity in mediating the metastasis suppressor activity of NM23-H1 (Hartsough et al., 2002) may need to be reexamined.

5.1.3. 3'-5' exonuclease activity of NM23-H1 is necessary to suppress *in vivo* spontaneous metastasis

To identify the relevant enzymatic activity to the metastasis suppression of NM23-H1, our laboratory has initiated the lung metastasis assay using 1205Lu cells stably transfected with NM23-H1 in nude mice. 1205Lu melanoma cells are suitable for this experiment due to its characteristics of high malignance with low background of NM23 expression. The spontaneous metastasis assay recapitulates most of the steps of cancer metastasis from primary tumor formation to metastatic lesion, representing the most powerful

model for studying metastasis. In the spontaneous metastasis assay, NM23-H1 transfected melanoma cells were subcutaneously injected into experimental mice. After the primary tumors were removed, mice were continually raised for another 3 months to form lung metastases.

Although 1205Lu cells are highly malignant, the spontaneous lung metastases still need long time (3 months) to complete. Since the cells are human-derived, they need acquire some genetic changes to adapt to their new mouse environment after they are injected subcutaneously. In this study, we observed that the wild-type NM23-H1 significantly inhibit the spontaneous lung metastasis of 1205Lu melanoma cells without affecting the growth of primary tumor. In the primary tumors of 1205Lu cells, genomic instability is associated with NM23-deficient stage. In light of our microarray data, some DNA repair genes such as Rad51, HUS1, MLH1, BRCA1 and FEN1 might be upregulated at H1-deficient primary sites. The DNA repair-like activity of NM23-H1 might oppose the genetic instability of the 1205Lu cells, thereby decreasing their spontaneous metastatic potential. Also it is recently reported that some genes involved in motility and anchorage independent growth (EDG2) are downregulated by NM23-H1 (Horak et al., 2007), supporting a role of NM23-H1 in suppressing early stage of metastasis. In the experimental metastasis models, since large numbers of 1205Lu cells are introduced directly into the vein, the cells have omitted the early rate-limiting steps of metastasis. Therefore, the metastasis-suppressing effect of NM23 is absent in the tail-vein injected mice. These results indicate that NM23-H1 may exert the suppressive effects on the earlier steps of metastases by inhibiting genomic instability at the primary sites.

In this study, site-directed mutageneses of NM23-H1 (E_5A-H1 and $K_{12}Q$-H1) demonstrate that 3'-5' exonuclease activity is necessary to suppress the spontaneous metastatic potential of 1205Lu melanoma cells. Originally, we hypothesized that the histidine kinase activity was not required for the metastasis suppressor function of NM23-H1 since the hisK-deficient mutation ($P_{96}S$) still maintained a significant anti-metastatic capacity. However, as discussed above, we gradually realized that the histidine kinase activity of NM23-H1 might be artifactual. The reason for why $P_{96}S$-H1 did not lose the metastasis-suppressing function is that $P_{96}S$-H1 still possesses significant 3'-

5' exonuclease activity. This further supports the necessities of the 3'-5' exonuclease activity for metastasis suppressor function of NM23-H1.

Interestingly, similar to the pattern observed in the metastasis assay, $K_{12}Q$ but not $P_{96}S$ mutant lost the effects of anti-metastatic progression exhibited by wild-type-H1 (Qingbei Zhang, Ph.D. dissertation 2006). This evidence further indicates that 3'-5' exonuclease activity is required to suppress the metastatic progression of melanoma cells. The effects of E_5A on the anti-metastatic progression would address the relevance of the 3'-5' exonuclease activity further, while the investigation (performed by Marián Novak) is currently underway.

5.1.4. The metastasis suppressor NM23-H1 is required for DNA repair

As known 3'-5' exonucleases are generally required for maintenance of genomic integrity, DNA repair activity represents a logical cellular function for the nuclease activities of NM23-H1 and NM23-H2. A previous study in *E. coli* provided an early indication that the NM23 homologue, *ndk*, was required for maintaining genomic integrity (Lu et al., 1995). However, the exact enzymatic activity(s) of *ndk* required for antimutator activity was not identified directly in that study. To measure the contribution of NM23-H1 to DNA repair, we have initiated experiments in the yeast *Saccharomyces cerevisiae*. The well-recognized characterizations of DNA repair pathways and mechanisms in yeast cell provide it an excellent genetic model to determine the role of NM23 proteins in DNA repair.

In this study, we have examined the contributions of *YNK1*, the yeast NM23 homologue, to genomic integrity in *S. cerevisiae*. Mutation rates were measured in a haploid *YNK1* knockout (*ynk1Δ*) strain using the standard *CAN1* forward mutation assay. Disruption of the *YNK1* gene in a haploid strain had no effect on viability, growth rate, spore formation, mating ability and morphology (Fukuchi et al., 1993). In this study, although the *YNK1* deletion had no effect on spontaneous mutation rate relative to wild-type, significantly increased mutations were observed in the *ynk1Δ* strain following treatment with UV radiation. These results suggest that *YNK1* deletion leads to a significant repair deficiency to UV-induced DNA damage. Mutation

spectra demonstrate the most UV-induced mutations in *ynk1Δ* strain are base substitutions and frameshifts. The high conservation between *YNK1* and NM23-H1 further indicates an anti-mutator function for the human homologue. The possible pathways could be: NM23 is directly involved in the repair process by recognizing, binding and excising modified or mutant DNA; NM23 interacts with other DNA repair mediators; NM23 regulates other gene expressions which are required for maintaining genomic integrity.

To identify possible interactions of *YNK1* with other DNA repair mediators, additional lesions were introduced into a variety of known DNA checkpoints and DNA repair genes (*DDC1*, *RAD17*, *MEC3*, *RAD27 and MSH2*) in the *ynk1Δ* background. The ability of *YNK1* to oppose UV-induced mutagenesis was negated in *ynk1Δ ddc1Δ*, *ynk1Δ rad17Δ* and *ynk1Δ mec3Δ* double mutants, suggesting *YNK1* is not likely to be involved in the 9-1-1 clamp-regulated pathway. However, the *ynk1Δ msh2Δ* strain exhibited an additive effect of the two deletions on UV-induced mutation rate, with a mutational spectrum of nucleotide misincorporations and single/double-base frameshifts events in the *msh2Δ* strain consistent with that of *ynk1Δ*. Taken together, these observations suggest involvement of *YNK1* in mismatch repair processes.

There are some DNA repair pathways that NM23 protein might be involved: 1) Based on the formation of a Schiff-base intermediate in NM23-H2, the residue Lys_{12} of NM23-H2 has been indicated to play a DNA glycosylase/lyase-like role (Postel et al., 2000). The Lys_{12} is a highly conserved residue, which is necessary for both NM23-H1 and NM23-H2 in their DNA cleavage activity. Since DNA glycosylase activity is a signature of base excision repair (BER), NM23 may play a role in BER in which the ε-amino group of lysine acts as a critical nucleophile in DNA cleavage reaction (Nash et al., 1997). 2) NM23 might be involved in mismatch repair pathway, since the deletion of *YNK1* and *MSH2* cause an additive phenotype of mutations following treatments of UV radiation with same mutational spectrum. 3) Upon the evidence that UV insult induces nuclear translocation and nuclear foci formation of NM23 proteins (Kaetzel et al., 2006), and that yeast cells lacking functional *YNK1* exhibits defective repair of UV damage, NM23 might

play a role in repairing UV-damaged DNA in nucleotide excision repair pathway.

In a summary, evidence is accumulating across a wide range of prokaryotic and eukaryotic organisms in support of a role for NM23-H1 in maintaining genomic integrity. Since NM23-H1 possesses multiple enzymatic activities, the mechanisms of action could be: 1) the 3'-5' exonuclease activity may play an important role in DNA repair, especially under genotoxic stress. 2) The 3'-5' exonuclease activity might excise a misincorporated nucleotide during DNA replication. 3) The NDPK activity maintains nucleotides balance, which might facilitate the fidelity of DNA polymerase by providing balanced nucleotides. Therefore, during tumor evolution, NM23 is necessary to reduce the generation and accumulation of mutations, by which it may inhibit cancer cells to acquire more genetic instability for metastatic development.

The eventual aim of this study is to utilize the metastasis suppressor NM23-H1 in the clinical setting as new therapeutic targets. To this end, our understandings that DNA repair activity of NM23-H1 is involved in its anti-metastatic mechanisms may contribute to new drug discoveries. For instance, metastasis may be suppressed or delayed by restoring the expression of NM23-H1, especially its 3'-5' exonuclease activity. The increased levels of DNA repair would result in a decrease in the accruement of mutations during metastasis progression, thereby reducing the metastasis incidence.

5.2. Future Perspectives

5.2.1. To measure the impact of NM23-H1 expression on mutation rates in mammalian cells.

The mutation rate is increased in Ndk-null *E. coli* and *ynk1Δ S. cerevisiae* strains, suggesting genes *Ndk* and *YNK1* (NM23 homologues) play important roles in opposing mutations. The yeast experimental paradigm of this project needs to be performed on NM23-deficient mammalian cells to test the role of NM23 as a guardian of genome integrity in mammalian cells.

Mouse embryo fibroblasts (MEFs) from NM23-M1 knockout mice are available in our lab. So, firstly, mutation rates at the hypoxanthine phosphribosyl-transferase (*hprt*) locus will be compared between MEFs derived from wild-type and NM23-M1 knockout mice under basal conditions. Toxic nucleoside analog 6-thioguanine (6-TG) will be used to select *hprt* mutant cell. Cells without the *hprt* mutation are poisoned by 6-TG, while mutant cells survive and form colonies. A known numbers of cells will be seeded in medium containing 6-TG to detect mutant cells, and medium without 6-TG can be used to obtain a plating efficiency. Mutant frequency is derived from the number of mutant colonies in selective medium and the number of colonies in non-selective medium (Glaab and Tindall, 1997). Mutation rates will also be compared under conditions of genotoxic stress. Etoposide and UV radiation can be firstly chosen to treat MEFs, since we have observed that -1- these two treatments induced translocation of NM23 proteins to subnuclear foci. -2- *YNK1* played an important role in UV damaged DNA response. There evidences suggest that genomic integrity would be compromised following treatment of UV radiation in NM23 deficient cells. Secondly, the degree of correlation between NM23-H1 status and mutation rate need to be determined in human melanoma cell lines. 1205Lu melanoma cells need to be examined due to the high malignancy and NM23 low background of the cells. The mutation rates can be measured under basal condition and genotoxic insult at the *hprt* locus, as described above. Or to circumvent the polyploidy of *hprt* gene, the mutation rates of 1205Lu cells can be also measured at Na^+/K^+ ATPase locus for ouabain resistant (Oua^R) mutations, as described previously (Elmore and Barrett, 1982). Thirdly, to identify the relevant biochemical activity of NM23-H1 mediating its anti-mutation function, mutator phenotype of NM23-M1 knockout MEFs and 1205Lu cells will be complemented with wild-type or mutant (E_5A, $K_{12}Q$, $P_{96}S$ and $H_{118}F$) NM23-H1. The complementary effects with NM23 variants will be related to their specific activities (NDPK and/or 3'-5' exonuclease).

5.2.2. To measure the extent to which deletion of *YNK1* affects a mismatch repair

To directly assess whether an ablation of *YNK1* causes a defect in mismatch repair (MMR), wild-type, *ynk1Δ, msh2Δ* and *ynk1Δ msh2Δ* strains will be transformed with an A:C mismatch-containing plasmid. Since the A:C mismatch resides in an *ADE8* gene, *ADE8* genes in the aforementioned strains need to be inactivated as previously described (Tishkoff et al., 1997) before plasmid transformation. The plasmid carries a functional *URA3* gene, so the transformants can be selected on SC-uracil plates. If the mismatch is corrected prior to DNA replication, the resulting colony is nonsectored and either red or white. However, if the mismatch is not repaired, then the two *ADE8* alleles segregate after DNA replication, resulting in a red/white sectored colony. The proportion of sectored colonies will positively reflect an extent of MMR defect. In the wild-type strain, only a small number of plasmids escape repair, yielding sectored colonies. The *msh2* mutant will be expected to yield about 60% of sectored colonies as previous described (Chen et al., 1999; Luhr et al., 1998). The impacts of the disruption of *YNK1* on MMR and the potentiating effects to *MSH2* gene will be reflected by the proportion of red/white sectored colonies in *ynk1Δ* and *ynk1Δ msh2Δ* strains respectively. This approach effectively examines the impacts of *ynk1* mutant on MMR defects *in vivo*.

REFFERENCES

Agarwal, R.P., Robison, B., and Parks, R.E., Jr. (1978). Nucleoside diphosphokinase from human erythrocytes. Methods in enzymology *51*, 376-386.

Ahmad, M., and Bussey, H. (1986). Yeast arginine permease: nucleotide sequence of the CAN1 gene. Current genetics *10*, 587-592.

Bailly, M., Bertrand, S., and Dore, J.F. (1993). Increased spontaneous mutation rates and prevalence of karyotype abnormalities in highly metastatic human melanoma cell lines. Melanoma research *3*, 51-61.

Berberich, S.J., and Postel, E.H. (1995). PuF/NM23-H2/NDPK-B transactivates a human c-myc promoter-CAT gene via a functional nuclease hypersensitive element. Oncogene *10*, 2343-2347.

Boissan, M., Wendum, D., Arnaud-Dabernat, S., Munier, A., Debray, M., Lascu, I., Daniel, J.Y., and Lacombe, M.L. (2005). Increased lung metastasis in transgenic NM23-Null/SV40 mice with hepatocellular carcinoma. Journal of the National Cancer Institute *97*, 836-845.

Calera, J.A., Choi, G.H., and Calderone, R.A. (1998). Identification of a putative histidine kinase two-component phosphorelay gene (CaHK1) in Candida albicans. Yeast (Chichester, England) *14*, 665-674.

Chambers, A.F., Groom, A.C., and MacDonald, I.C. (2002). Dissemination and growth of cancer cells in metastatic sites. Nat Rev Cancer *2*, 563-572.

Chen, C., Merrill, B.J., Lau, P.J., Holm, C., and Kolodner, R.D. (1999). Saccharomyces cerevisiae pol30 (proliferating cell nuclear antigen) mutations impair replication fidelity and mismatch repair. Molecular and cellular biology *19*, 7801-7815.

Cunningham, R.P. (1997). DNA glycosylases. Mutation research *383*, 189-196.

Dong, J.T., Suzuki, H., Pin, S.S., Bova, G.S., Schalken, J.A., Isaacs, W.B., Barrett, J.C., and Isaacs, J.T. (1996). Down-regulation of the KAI1 metastasis suppressor gene during the progression of human prostatic cancer infrequently involves gene mutation or allelic loss. Cancer research *56*, 4387-4390.

Dumas, C., Lascu, I., Morera, S., Glaser, P., Fourme, R., Wallet, V., Lacombe, M.L., Veron, M., and Janin, J. (1992). X-ray structure of nucleoside diphosphate kinase. The EMBO journal *11*, 3203-3208.

Elmore, E., and Barrett, J.C. (1982). Measurement of spontaneous mutation rates at the Na+/K+ ATPase locus (ouabain resistance) of human fibroblasts using improved growth conditions. Mutation research *97*, 393-404.

Fijalkowska, I.J., and Schaaper, R.M. (1996). Mutants in the Exo I motif of Escherichia coli dnaQ: defective proofreading and inviability due to error catastrophe. Proceedings of the National Academy of Sciences of the United States of America *93*, 2856-2861.

Freije, J.M., Blay, P., MacDonald, N.J., Manrow, R.E., and Steeg, P.S. (1997). Site-directed mutation of Nm23-H1. Mutations lacking motility suppressive capacity upon transfection are deficient in histidine-dependent protein phosphotransferase pathways in vitro. The Journal of biological chemistry *272*, 5525-5532.

Fukuchi, T., Nikawa, J., Kimura, N., and Watanabe, K. (1993). Isolation, overexpression and disruption of a Saccharomyces cerevisiae YNK gene encoding nucleoside diphosphate kinase. Gene *129*, 141-146.

Gasch, A.P., Huang, M., Metzner, S., Botstein, D., Elledge, S.J., and Brown, P.O. (2001). Genomic expression responses to DNA-damaging agents and the regulatory role of the yeast ATR homolog Mec1p. Molecular biology of the cell *12*, 2987-3003.

Glaab, W.E., and Tindall, K.R. (1997). Mutation rate at the hprt locus in human cancer cell lines with specific mismatch repair-gene defects. Carcinogenesis *18*, 1-8.

Goldsby, R.E., Lawrence, N.A., Hays, L.E., Olmsted, E.A., Chen, X., Singh, M., and Preston, B.D. (2001). Defective DNA polymerase-delta proofreading causes cancer susceptibility in mice. Nature medicine *7*, 638-639.

Harrington, J.J., and Lieber, M.R. (1994). Functional domains within FEN-1 and RAD2 define a family of structure-specific endonucleases: implications for nucleotide excision repair. Genes & development *8*, 1344-1355.

Hartsough, M.T., Morrison, D.K., Salerno, M., Palmieri, D., Ouatas, T., Mair, M., Patrick, J., and Steeg, P.S. (2002). Nm23-H1 metastasis suppressor phosphorylation of kinase suppressor of Ras via a histidine protein kinase pathway. The Journal of biological chemistry *277*, 32389-32399.

Hartsough, M.T., and Steeg, P.S. (2000). Nm23/nucleoside diphosphate kinase in human cancers. Journal of bioenergetics and biomembranes *32*, 301-308.

Ho, S.N., Hunt, H.D., Horton, R.M., Pullen, J.K., and Pease, L.R. (1989). Site-directed mutagenesis by overlap extension using the polymerase chain reaction. Gene *77*, 51-59.

Horak, C.E., Mendoza, A., Vega-Valle, E., Albaugh, M., Graff-Cherry, C., McDermott, W.G., Hua, E., Merino, M.J., Steinberg, S.M., Khanna, C.*, et al.* (2007). Nm23-H1 suppresses metastasis by inhibiting expression of the lysophosphatidic acid receptor EDG2. Cancer research *67*, 11751-11759.

Howlett, A.R., Petersen, O.W., Steeg, P.S., and Bissell, M.J. (1994). A novel function for the nm23-H1 gene: overexpression in human breast carcinoma cells leads to the formation of basement membrane and growth arrest. Journal of the National Cancer Institute *86*, 1838-1844.

Ji, L., Arcinas, M., and Boxer, L.M. (1995). The transcription factor, Nm23H2, binds to and activates the translocated c-myc allele in Burkitt's lymphoma. The Journal of biological chemistry *270*, 13392-13398.

Kaetzel, D.M., Zhang, Q., Yang, M., McCorkle, J.R., Ma, D., and Craven, R.J. (2006). Potential roles of 3'-5' exonuclease activity of NM23-H1 in DNA repair and malignant progression. Journal of bioenergetics and biomembranes *38*, 163-167.

Kath, R., Jambrosic, J.A., Holland, L., Rodeck, U., and Herlyn, M. (1991). Development of invasive and growth factor-independent cell variants from primary human melanomas. Cancer research *51*, 2205-2211.

Kauffman, E.C., Robinson, V.L., Stadler, W.M., Sokoloff, M.H., and Rinker-Schaeffer, C.W. (2003). Metastasis suppression: the evolving role of metastasis suppressor genes for regulating cancer cell growth at the secondary site. The Journal of urology *169*, 1122-1133.

Kim, H.L., Vander Griend, D.J., Yang, X., Benson, D.A., Dubauskas, Z., Yoshida, B.A., Chekmareva, M.A., Ichikawa, Y., Sokoloff, M.H., Zhan, P., *et al.* (2001). Mitogen-activated protein kinase kinase 4 metastasis suppressor gene expression is inversely related to histological pattern in advancing human prostatic cancers. Cancer research *61*, 2833-2837.

Kolodner, R. (1996). Biochemistry and genetics of eukaryotic mismatch repair. Genes & development *10*, 1433-1442.

Kondo, T., Matsumoto, K., and Sugimoto, K. (1999). Role of a complex containing Rad17, Mec3, and Ddc1 in the yeast DNA damage checkpoint pathway. Molecular and cellular biology *19*, 1136-1143.

Lacombe, M.L., Milon, L., Munier, A., Mehus, J.G., and Lambeth, D.O. (2000). The human Nm23/nucleoside diphosphate kinases. Journal of bioenergetics and biomembranes *32*, 247-258.

Lascu, I., Schaertl, S., Wang, C., Sarger, C., Giartosio, A., Briand, G., Lacombe, M.L., and Konrad, M. (1997). A point mutation of human nucleoside diphosphate kinase A found in aggressive neuroblastoma affects protein folding. The Journal of biological chemistry *272*, 15599-15602.

Lascu, L., Giartosio, A., Ransac, S., and Erent, M. (2000). Quaternary structure of nucleoside diphosphate kinases. Journal of bioenergetics and biomembranes *32*, 227-236.

Lau, P.J., Flores-Rozas, H., and Kolodner, R.D. (2002). Isolation and characterization of new proliferating cell nuclear antigen (POL30) mutator mutants that are defective in DNA mismatch repair. Molecular and cellular biology *22*, 6669-6680.

Levit, M.N., Abramczyk, B.M., Stock, J.B., and Postel, E.H. (2002). Interactions between Escherichia coli nucleoside-diphosphate kinase and DNA. The Journal of biological chemistry *277*, 5163-5167.

Liu, B., Maul, R.S., and Kaetzel, D.M., Jr. (1996). Repression of platelet-derived growth factor A-chain gene transcription by an upstream silencer element. Participation by sequence-specific single-stranded DNA-binding proteins. The Journal of biological chemistry *271*, 26281-26290.

Loeb, L.A. (1991). Mutator phenotype may be required for multistage carcinogenesis. Cancer research *51*, 3075-3079.

Loeb, L.A. (2001). A mutator phenotype in cancer. Cancer research *61*, 3230-3239.

Lombardi, D., Lacombe, M.L., and Paggi, M.G. (2000). nm23: unraveling its biological function in cell differentiation. Journal of cellular physiology *182*, 144-149.

Longhese, M.P., Paciotti, V., Fraschini, R., Zaccarini, R., Plevani, P., and Lucchini, G. (1997). The novel DNA damage checkpoint protein ddc1p is phosphorylated periodically during the cell cycle and in response to DNA damage in budding yeast. The EMBO journal *16*, 5216-5226.

Lu, Q., Zhang, X., Almaula, N., Mathews, C.K., and Inouye, M. (1995). The gene for nucleoside diphosphate kinase functions as a mutator gene in Escherichia coli. Journal of molecular biology *254*, 337-341.

Luhr, B., Scheller, J., Meyer, P., and Kramer, W. (1998). Analysis of in vivo correction of defined mismatches in the DNA mismatch repair mutants msh2, msh3 and msh6 of Saccharomyces cerevisiae. Mol Gen Genet *257*, 362-367.

Ma, D., McCorkle, J.R., and Kaetzel, D.M. (2004). The metastasis suppressor NM23-H1 possesses 3'-5' exonuclease activity. The Journal of biological chemistry *279*, 18073-18084.

Ma, D., Xing, Z., Liu, B., Pedigo, N.G., Zimmer, S.G., Bai, Z., Postel, E.H., and Kaetzel, D.M. (2002). NM23-H1 and NM23-H2 repress transcriptional activities of nuclease-hypersensitive elements in the platelet-derived growth factor-A promoter. The Journal of biological chemistry *277*, 1560-1567.

MacDonald, N.J., De la Rosa, A., Benedict, M.A., Freije, J.M., Krutsch, H., and Steeg, P.S. (1993). A serine phosphorylation of Nm23, and not its nucleoside diphosphate kinase activity, correlates with suppression of tumor metastatic potential. The Journal of biological chemistry *268*, 25780-25789.

MacDonald, N.J., Freije, J.M., Stracke, M.L., Manrow, R.E., and Steeg, P.S. (1996). Site-directed mutagenesis of nm23-H1. Mutation of proline 96 or serine 120 abrogates its motility inhibitory activity upon transfection into human breast carcinoma cells. The Journal of biological chemistry *271*, 25107-25116.

Majka, J., and Burgers, P.M. (2003). Yeast Rad17/Mec3/Ddc1: a sliding clamp for the DNA damage checkpoint. Proceedings of the National Academy of Sciences of the United States of America *100*, 2249-2254.

Marsischky, G.T., Filosi, N., Kane, M.F., and Kolodner, R. (1996). Redundancy of Saccharomyces cerevisiae MSH3 and MSH6 in MSH2-dependent mismatch repair. Genes & development *10*, 407-420.

McCullough, A.K., Dodson, M.L., and Lloyd, R.S. (1999). Initiation of base excision repair: glycosylase mechanisms and structures. Annual review of biochemistry *68*, 255-285.

McDermott, W.G., Boissan, M., Lacombe, M.L., Steeg, P.S., and Horak, C.E. (2007). Nm23-H1 homologs suppress tumor cell motility and anchorage independent growth. Clinical & experimental metastasis.

McGregor, W.G. (1999). DNA repair, DNA replication, and UV mutagenesis. The journal of investigative dermatology Symposium proceedings / the Society for Investigative Dermatology, Inc *4*, 1-5.

Morera, S., Lacombe, M.L., Xu, Y., LeBras, G., and Janin, J. (1995). X-ray structure of human nucleoside diphosphate kinase B complexed with GDP at 2 A resolution. Structure *3*, 1307-1314.

Morrison, A., Johnson, A.L., Johnston, L.H., and Sugino, A. (1993). Pathway correcting DNA replication errors in Saccharomyces cerevisiae. The EMBO journal *12*, 1467-1473.

Myeroff, L.L., and Markowitz, S.D. (1993). Increased nm23-H1 and nm23-H2 messenger RNA expression and absence of mutations in colon carcinomas of low and high metastatic potential. Journal of the National Cancer Institute *85*, 147-152.

Nash, H.M., Lu, R., Lane, W.S., and Verdine, G.L. (1997). The critical active-site amine of the human 8-oxoguanine DNA glycosylase, hOgg1: direct identification, ablation and chemical reconstitution. Chemistry & biology *4*, 693-702.

Nelson, J.R., Lawrence, C.W., and Hinkle, D.C. (1996). Thymine-thymine dimer bypass by yeast DNA polymerase zeta. Science (New York, NY *272*, 1646-1649.

Nguyen, D.X., and Massague, J. (2007). Genetic determinants of cancer metastasis. Nat Rev Genet *8*, 341-352.

Nowell, P.C. (1976). The clonal evolution of tumor cell populations. Science (New York, NY *194*, 23-28.

Odintsova, E., Sugiura, T., and Berditchevski, F. (2000). Attenuation of EGF receptor signaling by a metastasis suppressor, the tetraspanin CD82/KAI-1. Curr Biol *10*, 1009-1012.

Ouatas, T., Salerno, M., Palmieri, D., and Steeg, P.S. (2003). Basic and translational advances in cancer metastasis: Nm23. Journal of bioenergetics and biomembranes *35*, 73-79.

Palmieri, D., Horak, C.E., Lee, J.H., Halverson, D.O., and Steeg, P.S. (2006). Translational approaches using metastasis suppressor genes. Journal of bioenergetics and biomembranes *38*, 151-161.

Paulovich, A.G., Armour, C.D., and Hartwell, L.H. (1998). The Saccharomyces cerevisiae RAD9, RAD17, RAD24 and MEC3 genes are required for tolerating irreparable, ultraviolet-induced DNA damage. Genetics *150*, 75-93.

Postel, E.H. (1998). NM23-NDP kinase. The international journal of biochemistry & cell biology *30*, 1291-1295.

Postel, E.H. (1999). Cleavage of DNA by human NM23-H2/nucleoside diphosphate kinase involves formation of a covalent protein-DNA complex. The Journal of biological chemistry *274*, 22821-22829.

Postel, E.H. (2003). Multiple biochemical activities of NM23/NDP kinase in gene regulation. Journal of bioenergetics and biomembranes *35*, 31-40.

Postel, E.H., Abramczyk, B.A., Gursky, S.K., and Xu, Y. (2002). Structure-based mutational and functional analysis identify human NM23-H2 as a multifunctional enzyme. Biochemistry *41*, 6330-6337.

Postel, E.H., Abramczyk, B.M., Levit, M.N., and Kyin, S. (2000). Catalysis of DNA cleavage and nucleoside triphosphate synthesis by NM23-H2/NDP kinase share an active site that implies a DNA repair function. Proceedings of the National Academy of Sciences of the United States of America *97*, 14194-14199.

Qiu, J., Li, X., Frank, G., and Shen, B. (2001). Cell cycle-dependent and DNA damage-inducible nuclear localization of FEN-1 nuclease is consistent with its dual functions in DNA replication and repair. The Journal of biological chemistry *276*, 4901-4908.

Rosengard, A.M., Krutzsch, H.C., Shearn, A., Biggs, J.R., Barker, E., Margulies, I.M., King, C.R., Liotta, L.A., and Steeg, P.S. (1989). Reduced Nm23/Awd protein in tumour metastasis and aberrant Drosophila development. Nature *342*, 177-180.

Sabbioneda, S., Minesinger, B.K., Giannattasio, M., Plevani, P., Muzi-Falconi, M., and Jinks-Robertson, S. (2005). The 9-1-1 checkpoint clamp physically interacts with polzeta and is partially required for spontaneous polzeta-dependent mutagenesis in Saccharomyces cerevisiae. The Journal of biological chemistry *280*, 38657-38665.

Sadek, C.M., Jimenez, A., Damdimopoulos, A.E., Kieselbach, T., Nord, M., Gustafsson, J.A., Spyrou, G., Davis, E.C., Oko, R., van der Hoorn, F.A.*, et al.* (2003). Characterization of human thioredoxin-like 2. A novel microtubule-binding thioredoxin expressed predominantly in the cilia of lung airway epithelium and spermatid manchette and axoneme. The Journal of biological chemistry *278*, 13133-13142.

Salerno, M., Ouatas, T., Palmieri, D., and Steeg, P.S. (2003). Inhibition of signal transduction by the nm23 metastasis suppressor: possible mechanisms. Clinical & experimental metastasis *20*, 3-10.

Shen, B., Nolan, J.P., Sklar, L.A., and Park, M.S. (1996). Essential amino acids for substrate binding and catalysis of human flap endonuclease 1. The Journal of biological chemistry *271*, 9173-9176.

Shevelev, I.V., and Hubscher, U. (2002). The 3' 5' exonucleases. Nature reviews *3*, 364-376.

Siclari, V.A., Guise, T.A., and Chirgwin, J.M. (2006). Molecular interactions between breast cancer cells and the bone microenvironment drive skeletal metastases. Cancer metastasis reviews *25*, 621-633.

Sieber, O.M., Heinimann, K., and Tomlinson, I.P. (2003). Genomic instability--the engine of tumorigenesis? Nat Rev Cancer *3*, 701-708.

Sporn, M.B. (1996). The war on cancer. Lancet *347*, 1377-1381.

Sreerama, N., and Woody, R.W. (2000). Estimation of protein secondary structure from circular dichroism spectra: comparison of CONTIN, SELCON, and CDSSTR methods with an expanded reference set. Analytical biochemistry *287*, 252-260.

Steeg, P.S. (2003). Metastasis suppressors alter the signal transduction of cancer cells. Nat Rev Cancer *3*, 55-63.

Steeg, P.S., Bevilacqua, G., Kopper, L., Thorgeirsson, U.P., Talmadge, J.E., Liotta, L.A., and Sobel, M.E. (1988). Evidence for a novel gene associated with low tumor metastatic potential. Journal of the National Cancer Institute *80*, 200-204.

Teng, D.H., Perry, W.L., 3rd, Hogan, J.K., Baumgard, M., Bell, R., Berry, S., Davis, T., Frank, D., Frye, C., Hattier, T.*, et al.* (1997). Human mitogen-activated protein kinase kinase 4 as a candidate tumor suppressor. Cancer research *57*, 4177-4182.

Thelen, M.P., Venclovas, C., and Fidelis, K. (1999). A sliding clamp model for the Rad1 family of cell cycle checkpoint proteins. Cell *96*, 769-770.

Tishkoff, D.X., Filosi, N., Gaida, G.M., and Kolodner, R.D. (1997). A novel mutation avoidance mechanism dependent on S. cerevisiae RAD27 is distinct from DNA mismatch repair. Cell *88*, 253-263.

Tomayko, M.M., and Reynolds, C.P. (1989). Determination of subcutaneous tumor size in athymic (nude) mice. Cancer chemotherapy and pharmacology *24*, 148-154.

Webb, P.A., Perisic, O., Mendola, C.E., Backer, J.M., and Williams, R.L. (1995). The crystal structure of a human nucleoside diphosphate kinase, NM23-H2. Journal of molecular biology *251*, 574-587.

Welch, D.R. (1997). Technical considerations for studying cancer metastasis in vivo. Clinical & experimental metastasis *15*, 272-306.

Yamada, S.D., Hickson, J.A., Hrobowski, Y., Vander Griend, D.J., Benson, D., Montag, A., Karrison, T., Huo, D., Rutgers, J., Adams, S.*, et al.* (2002). Mitogen-activated protein kinase kinase 4 (MKK4) acts as a metastasis suppressor gene in human ovarian carcinoma. Cancer research *62*, 6717-6723.

Yang, X., Welch, D.R., Phillips, K.K., Weissman, B.E., and Wei, L.L. (1997). KAI1, a putative marker for metastatic potential in human breast cancer. Cancer letters *119*, 149-155.

Yoon, J.H., Singh, P., Lee, D.H., Qiu, J., Cai, S., O'Connor, T.R., Chen, Y., Shen, B., and Pfeifer, G.P. (2005). Characterization of the 3' --> 5' exonuclease activity found in human nucleoside diphosphate kinase 1 (NDK1) and several of its homologues. Biochemistry *44*, 15774-15786.

Zhang, Q. (2006). Molecular mechanisms that mediate metastasis suppressor activity of NM23-H1. Dissertation at University of Kentucky

VITA

PERSONAL INFORMATION

Date and Place of Birth   4/20/1976   Qinghai, China

EDUCATION

Ph.D. Candidate, Pharmacology, University of Kentucky, 2004-present

M.D., Clinical Medicine, Shandong University, China, 1998

RESEARCH & TEACHING EXPERIENCE

2002 - 2008	Graduate Research Fellow,
	Department of Pharmacology,
	University of Kentucky
1998 - 2001	Department of Physiology,
	Shandong University, CHINA

PUBLICATIONS

Kaetzel, D.M., Zhang, Q., **Yang, M.**, McCorle, J.R., Ma, D., and Craven, R.J. (2006). Potential roles of 3'-5' exonuclease activity of NM23-H1 in DNA repair and malignant progression. *J Bioenerg Biomembr* 38, 163-167.

Zhang, Q., **Yang, M.**, Novak, M., McCorkle, J.R., and Kaetzel, D.M. Dissociation of the nucleoside diphosphate kinase, histidine kinase, and 3'-5' exonuclease activities of NM23-H1 by site-directed mutagenesis. In preparation for *Cancer Res.* First three authors are co-firsts.

CONFERENCE ABSTRACTS

Yang, M., Jarrett, S., Craven, R.J., and Kaetzel, D.M. Analysis of DNA repair activity for *YNK1*, the yeast *Saccharomyces cerevisiae* homologue of the metastasis suppressor NM23. 99th AACR Annual Meeting, Apr. 12-16, 2008, San Diego

McCorkle, J.R.**, Yang, M.** and Kaetzel, D.M. Site-directed mutagenesis identifies residues necessary for multiple enzymatic activities of the metastasis suppressor NM23-H1. 98th AACR Annual Meeting, April 14-18, 2007, Los Angeles

Zhang, Q., McCorkle, J.R., **Yang, M.** and Kaetzel, D.M. The nucleoside diphosphate kinase and 3'-5' exonuclease activities of NM23-H1 may contribute to suppression of metastasis in melanoma cells: a complementation approach. Metastasis Society Congress, Sep. 2006, Tokushima, Japan

Yang, M. and Kaetzel, D.M. Analysis of DNA repair activity for *YNK1*, the yeast homologue of the metastasis suppressor NM23. 97th AACR Annual Meeting, Apr. 1-5, 2006, Washington, DC

Zhang, Q., **Yang, M.**, McCorkle, J.R., Craven, R.J., Ma, D., and Kaetzel, D.M., Potential roles of 3'-5' exonuclease activity of NM23-H1 in DNA repair and malignant progression. *NDP Kinase/NM23* International Congress, Oct. 17-19, 2005, Ceinge, Naples, Italy

MEMBERSHIPS

Associate Member, American Association for Cancer Research

Associate Member, American Association for the Advancement of Science

Mengmeng Yang

May 28, 2008